

Qudit Classical Shadow Tomography in Arbitrary Finite Dimensions via Minimal IC-POVMs from Weyl–Heisenberg Orbits

Xiuwu Zhu¹ and Yu Wang^{1,*}

¹*Beijing Key Laboratory of Topological Statistics and Applications for Complex Systems,
Beijing Institute of Mathematical Sciences and Applications, Beijing 101408, China.*

Efficient characterization and learning of quantum states in finite-dimensional systems is a central task in quantum information science. Symmetric informationally complete POVMs (SIC-POVMs) offer optimal tomographic performance, but their existence in general dimensions remains an open problem in quantum information theory. A SIC-POVM is constructed from a single fiducial state whose Weyl–Heisenberg orbit forms a highly symmetric, informationally complete set. In this work, we resolve a relaxed yet fundamental version of this problem by proving that for every finite dimension, there always exists a fiducial state whose Weyl–Heisenberg orbit yields a minimal IC-POVM, without symmetry assumptions. Our key contribution is a complete diagonalization of the associated Gram matrix: its eigenvectors form tensor products of Fourier basis states, and its eigenvalues are given by the two-dimensional discrete Fourier transform of the fiducial state’s autocorrelation function. This spectral structure enables explicit reconstruction formulas and reveals several classes of fiducial states cannot generate IC-POVMs or the more restrictive SIC-POVMs. Leveraging the constructed orbits, we propose a classical shadow tomography framework for qudit systems, where the minimum eigenvalue directly governs the estimation variance. Our method achieves sampling efficiency comparable to SIC-POVMs while significantly reducing computational complexity to obtain the fiducial state. Numerical simulations confirm that in high dimensions, randomly chosen fiducial states yield IC-POVMs with high probability, demonstrating both theoretical universality and practical feasibility.

I. INTRODUCTION

The complete characterization and efficient learning of quantum states stands as a central challenge in quantum information science. A general d -dimensional quantum state is described by a density matrix $\rho \in \mathbb{C}^{d \times d}$ [1], which contains $d^2 - 1$ independent real parameters and encodes all physically accessible information about the system. Recovering this information via quantum state tomography requires a measurement scheme that provides at least $d^2 - 1$ linearly independent statistics—exactly the minimal requirement satisfied by an informationally complete positive operator-valued measure (IC-POVM) [2].

Beyond enabling full state reconstruction, information completeness also underpin modern approaches such as classical shadow tomography [3], which aims to predict a large number of observable properties from a limited set of randomized measurements. Recent advances have generalized the classical shadow tomography framework from using randomly multiple sets of orthonormal projective measurements [3–13] to employing a single IC-POVM [14–17].

In this work, we answer this question affirmatively by constructing minimal IC-POVMs based on Weyl–Heisenberg orbits, and demonstrating their effectiveness in classical shadow estimation. Our results show that these fixed measurements not only admit efficient reconstruction formulas but also achieve sample and post-processing complexity comparable to traditional randomized shadow schemes.

The emergence of **classical shadow tomography** has transformed this landscape by reconceptualizing the tomographic problem: rather than pursuing complete state reconstruction, shadow protocols focus on efficiently estimating specific observable expectation values with polynomial measurement scaling. This paradigm shift reduces resource requirements from exponential to polynomial, making tomography tractable for systems of practical interest. However, the efficacy of shadow tomography critically depends on the underlying measurement ensemble, specifically requiring **informationally complete positive operator-valued measures** (IC-POVMs) that satisfy two stringent criteria: spanning the complete space of Hermitian operators while maintaining exactly d^2 elements for optimal efficiency.

Among the most celebrated candidates for such measurements are **symmetric informationally complete POVMs** (SIC-POVMs), which emerge from the orbit structure of the **Weyl–Heisenberg group**—the discrete analog of phase-space displacement operators in quantum optics. When a fiducial state satisfies the restrictive SIC condition $|\langle \psi_i | \psi_j \rangle|^2 = (d\delta_{ij} + 1)/(d + 1)$, its Weyl–Heisenberg orbit generates a measurement ensemble that simultaneously achieves informational completeness and forms a unitary 2-design. Such configurations are provably optimal for tomographic reconstruction, minimizing estimation variance while providing robust performance across diverse quantum states.

Despite their theoretical elegance, **SIC-POVMs face a fundamental constructibility crisis**. Zauner’s conjecture, which asserts their existence across all finite dimensions, remains unproven after decades of intensive investigation. Analytical constructions exist only for se-

* wangyu@bimsa.cn

lect low dimensions, while numerical solutions have been identified up to dimension 181 through exhaustive computational searches. The deep mathematical connections to algebraic number theory—particularly aspects of Hilbert’s twelfth problem and class field extensions—suggest that universal SIC-POVM constructions may be intrinsically intractable. Recent work has established that resolving Stark’s conjecture in number theory would imply Zauner’s conjecture, highlighting the profound mathematical depth underlying this problem.

This existence uncertainty creates a critical bottleneck for scalable quantum technologies. While SIC-POVMs represent the theoretical gold standard for quantum tomography, their non-constructive nature prevents deployment in realistic high-dimensional quantum systems where efficient state characterization is most urgently needed. The stringent symmetry requirements that endow SIC-POVMs with optimality simultaneously render them inaccessible for practical implementation.

This work addresses a fundamental question that reframes the tomographic landscape: **Can we achieve informational completeness without demanding perfect geometric symmetry?** We investigate whether the Weyl-Heisenberg orbit of a generic fiducial state—one that does not necessarily satisfy the restrictive SIC condition—can nevertheless span the operator space and form a minimal IC-POVM suitable for shadow tomography.

Our approach represents a paradigmatic shift from **geometric regularity to algebraic completeness**. Rather than enforcing uniform inner product magnitudes and geometric constraints, we determine informational completeness purely through the spectral properties of the associated **Gram matrix** constructed from fiducial state overlaps. When this matrix achieves full rank, the corresponding Weyl-Heisenberg orbit spans the operator space, yielding an IC-POVM with well-defined reconstruction guarantees.

We establish both theoretical foundations and constructive results that resolve the dimensional scaling problem for quantum tomography. Our main contributions include: (1) explicit fiducial state constructions that guarantee informational completeness across arbitrary dimensions, (2) comprehensive characterization of failure modes that prevent IC-POVM formation, (3) performance analysis demonstrating near-optimal reconstruction variance, and (4) optimization protocols that achieve SIC-POVM-level performance without requiring exact symmetry conditions.

These results demonstrate that the pursuit of perfect symmetry, while mathematically compelling, may impose unnecessary constraints on practical quantum tomography. By relaxing structural requirements while preserving informational completeness, we enable scalable shadow tomography protocols that bridge theoretical optimality with experimental reality, opening new pathways for quantum state characterization in high-dimensional and near-term quantum architectures.

II. PRELIMINARIES

Definition 1 (Fourier transformed basis state $|\mathcal{F}_m\rangle$). *The Fourier transform plays a central role in quantum computing. In any d -dimensional Hilbert space, the Fourier-transformed basis states are defined as*

$$|\mathcal{F}_m\rangle = \frac{1}{\sqrt{d}} \sum_{j=0}^{d-1} \omega^{mj} |j\rangle, \quad \omega = e^{2\pi i/d}, \quad m = 0, \dots, d-1. \quad (1)$$

These basis states form an orthonormal basis and will later play a central role in the spectral decomposition of Gram matrices associated with Weyl-Heisenberg orbits.

Definition 2 (Weyl-Heisenberg group). *The Weyl-Heisenberg group is a unitary group acting on a d -dimensional Hilbert space, generated by the shift operator X and the phase operator Z , defined as*

$$X = \sum_{j=0}^{d-1} |j+1 \bmod d\rangle \langle j|, \quad Z = \sum_{j=0}^{d-1} \omega^j |j\rangle \langle j|. \quad (2)$$

These operators satisfy the commutation relation $ZX = \omega XZ$, and generate a full set of displacement operators:

$$M_{jk} = X^j Z^k, \quad \text{for } j, k \in \mathbb{Z}_d. \quad (3)$$

The Weyl-Heisenberg group can be viewed as a natural generalization of the Pauli group from qubit systems to arbitrary finite dimensions, providing a discrete analog of phase-space translations in finite quantum systems.

Remark. Strictly speaking, the full Weyl-Heisenberg group includes an additional global phase: $\{\omega^\ell X^j Z^k \mid \ell, j, k \in \mathbb{Z}_d\}$, ensuring closure under group multiplication. In this work, we omit the global phase factor as it does not affect the Gram matrix structure or the informational completeness of the resulting POVMs.

Definition 3 (Weyl-Heisenberg orbit). *Given a fiducial quantum state $|\phi\rangle \in \mathcal{H}_d$, the Weyl-Heisenberg orbit of $|\phi\rangle$ is the set*

$$\mathcal{O}_\phi = \{X^j Z^k |\phi\rangle \mid j, k \in \mathbb{Z}_d\}, \quad (4)$$

consisting of d^2 states generated by applying all Weyl-Heisenberg displacement operators to $|\phi\rangle$.

To simplify notation, we label each operator M_{jk} by a single index $\alpha \in \{0, \dots, d^2 - 1\}$ using $\alpha = jd + k$, so that

$$M_\alpha := M_{jk} = X^j Z^k, \quad \text{with } \alpha = jd + k. \quad (5)$$

Definition 4 (Gram matrix $\mathcal{G}_{|\phi\rangle}$ for Weyl-Heisenberg orbit). *Let $|\phi\rangle = \sum_{k=0}^{d-1} a_k |k\rangle \in \mathcal{H}_d$ be a normalized quantum state. The associated Gram matrix $\mathcal{G}_{|\phi\rangle} \in \mathbb{C}^{d^2 \times d^2}$ is defined by the squared overlaps between elements of the Weyl-Heisenberg orbit:*

$$\mathcal{G}_{|\phi\rangle} = (|\langle \phi_\alpha | \phi_\beta \rangle|^2)_{\alpha, \beta=0}^{d^2-1}, \quad (6)$$

where $|\phi_\alpha\rangle = M_\alpha|\phi\rangle$.

This matrix is real, symmetric, and hence Hermitian. Explicitly, it can also be expressed as

$$\mathcal{G}_{|\phi\rangle} = \sum_{m,n,p,q=0}^{d-1} |\langle\phi|(X^m Z^n)^\dagger (X^p Z^q)|\phi\rangle|^2 \cdot |mn\rangle\langle pq|. \quad (7)$$

Matrix form. For clarity, the Gram matrix can be written as

$$\mathcal{G}_{|\phi\rangle} = \begin{pmatrix} |\langle\phi_0|\phi_0\rangle|^2 & |\langle\phi_0|\phi_1\rangle|^2 & \cdots & |\langle\phi_0|\phi_{d^2-1}\rangle|^2 \\ |\langle\phi_1|\phi_0\rangle|^2 & |\langle\phi_1|\phi_1\rangle|^2 & \cdots & |\langle\phi_1|\phi_{d^2-1}\rangle|^2 \\ \vdots & \vdots & \ddots & \vdots \\ |\langle\phi_{d^2-1}|\phi_0\rangle|^2 & |\langle\phi_{d^2-1}|\phi_1\rangle|^2 & \cdots & |\langle\phi_{d^2-1}|\phi_{d^2-1}\rangle|^2 \end{pmatrix}$$

Property 1 (Tight frame property for any Weyl–Heisenberg orbit). *Let $\{|\phi_k\rangle\}_{k=0}^{d^2-1}$ be the set of quantum states obtained by the action of the Weyl–Heisenberg group on a fiducial state $|\phi\rangle$. Then this set forms a tight frame with frame operator*

$$\sum_{k=0}^{d^2-1} |\phi_k\rangle\langle\phi_k| = d \cdot I. \quad (8)$$

A detailed proof is provided in Appendix A.

Method 1 (Fiducial state for SIC-POVM and Zauner’s conjecture). *A symmetric informationally complete POVM (SIC-POVM) in a d -dimensional Hilbert space is a set of d^2 subnormalized projectors $\{|\phi_k\rangle\langle\phi_k|/d\}_{k=0}^{d^2-1}$, such that the pairwise overlaps between the normalized vectors $|\phi_k\rangle$ satisfy*

$$|\langle\phi_k|\phi_{k'}\rangle|^2 = \frac{1}{d+1}, \quad \text{for all } k \neq k'. \quad (9)$$

Equivalently, if the Gram matrix of a fiducial state $|\phi\rangle$ satisfies

$$\mathcal{G}_{|\phi\rangle} = \frac{1}{d+1} (\delta_{\alpha\beta} \cdot (d+1) + (1 - \delta_{\alpha\beta})), \quad (10)$$

then the corresponding Weyl–Heisenberg orbit forms a SIC-POVM with elements $\{|\phi_k\rangle\langle\phi_k|/d\}_{k=0}^{d^2-1}$.

The construction of SIC-POVMs [18] has been recognized by Horodecki et al. as one of the five central open problems in quantum information theory [19], specifically concerning the existence of a SIC-POVM in every finite dimension d . The prevailing approach is to search for a fiducial state that satisfies Eq. (9), which then generates the desired structure via its Weyl–Heisenberg orbit. Zauner’s conjecture posits that such a fiducial state exists for all d , and while both analytical and numerical solutions have been found for certain dimensions, a general proof remains elusive. Moreover, the problem reveals intriguing connections to algebraic number theory, particularly to aspects of Hilbert’s twelfth problem [20, 21].

Notably, a recent QIP 2025 talk highlighted that a proof of the Stark’s conjecture in number theory would imply the validity of Zauner’s conjecture [22].

Once a suitable fiducial state is identified, its Weyl–Heisenberg orbit yields a set of d^2 equiangular lines in complex Hilbert space [23], offering valuable insights into the geometry of quantum state space [24]. By contrast, in real inner product spaces, the maximum number of equiangular lines with a fixed angle scales only as $O(d)$, underscoring a sharp distinction between the complex and real settings [25].

Motivated by this, we investigate whether relaxing the symmetry condition inherent in SIC-POVMs is sufficient to achieve informational completeness. Specifically, we examine the existence of fiducial states for informationally complete POVMs (IC-POVMs) without the stringent symmetry constraints. If no such fiducial state exists for an IC-POVM for special dimension d , it would imply the non-existence of a fiducial state for a SIC-POVM, given that SIC-POVMs are a subset of IC-POVMs with additional symmetry properties.

Method 2 (Fiducial state for IC-POVM). *If the Gram matrix $\mathcal{G}_{|\phi\rangle}$ defined in Eq. (6) has a nonzero determinant, then the d^2 states generated by acting the Weyl–Heisenberg group on the fiducial state $|\phi\rangle$ can form an informationally complete POVM (IC-POVM).*

This criterion was rigorously established in recent work [26]. According to Property 1, if $\det(\mathcal{G}_{|\phi\rangle}) \neq 0$, then the set $\{|\phi_k\rangle\langle\phi_k|/d\}_{k=0}^{d^2-1}$ forms a minimal IC-POVM. The POVM condition is satisfied because each element is normalized and the set sums to the identity. Moreover, since the set consists of d^2 rank-one projectors spanning the operator space, it is minimal in the sense of informational completeness.

III. RESULTS

We are therefore interested in how the choice of $|\phi\rangle$ affects the structure and determinant of the Gram matrix $\mathcal{G}_{|\phi\rangle}$.

Theorem 1 (Diagonalization of the Gram Matrix). *The complete set of eigenvectors of the $d^2 \times d^2$ Gram matrix $\mathcal{G}_{|\phi\rangle}$ is given by the tensor products of the Fourier basis states:*

$$|\Phi_{mn}\rangle = |\mathcal{F}_m\rangle \otimes |\mathcal{F}_n\rangle, \quad (11)$$

where $m, n = 0, \dots, d-1$, and $|\mathcal{F}_m\rangle$ is the m -th Fourier transformed states defined in Eq. (1). These d^2 vectors form an orthonormal eigenbasis of $\mathcal{G}_{|\phi\rangle}$.

Each eigenvector $|\Phi_{mn}\rangle$ corresponds to the eigenvalue

$$\lambda_{mn} = \sum_{j=0}^{d-1} \sum_{k=0}^{d-1} |\langle\phi|X^j Z^k|\phi\rangle|^2 \cdot \omega^{mj+nk}. \quad (12)$$

A specified expression is provided in Eq. (B11).

The proof of this result, including the derivation of Eq. (12), is provided in Appendix B.

This formula reveals that the eigenvalues λ_{mn} are precisely the two-dimensional discrete Fourier transform (2D DFT) of the matrix $|\langle\phi|X^jZ^k|\phi\rangle|^2$. In other words, the Gram matrix spectrum is determined by the interference pattern encoded in the autocorrelation structure of $|\phi\rangle$ under the Weyl–Heisenberg action. This structure underpins the connection between the spectral properties of the Gram matrix and the Fourier analysis on the discrete phase space.

Theorem 2 (Existence of informationally complete fiducial states in all dimensions). *For every positive integer d , there exists a pure state $|\phi\rangle \in \mathbb{C}^d$ such that the Gram matrix $\mathcal{G}_{|\phi\rangle}$, constructed from the Weyl–Heisenberg orbit $\{M_\alpha|\phi\rangle\}_{\alpha \in \mathbb{Z}_d \times \mathbb{Z}_d}$, is full rank. Consequently, this orbit defines an informationally complete POVM (IC-POVM).*

Moreover:

- For all even d , the fiducial state

$$|\phi\rangle = \frac{1}{\sqrt{d}}(|0\rangle + \sum_{j=1}^{d-1} \zeta^j |j\rangle), \quad (13)$$

where $\zeta = e^{2\pi i/(d+1)}$, generates an IC-POVM.

- For all odd d , the fiducial state

$$|\phi\rangle = \frac{1}{\sqrt{d-1}} \sum_{j \neq j_0} |j\rangle, \quad (14)$$

with any fixed $j_0 \in \{0, \dots, d-1\}$, also generates an IC-POVM.

The minimal eigenvalue of the associated Gram matrix is strictly positive in both cases. For odd d , it satisfies the asymptotic bound

$$\lambda_{\min} = 2d \left(1 - \cos\left(\frac{\pi}{d}\right)\right) = \frac{\pi^2}{d} + O(d^{-3}).$$

Remark 1. *In the case $d = 2$, our analysis yields a complete characterization of all fiducial states that generate an IC-POVM via Weyl–Heisenberg orbits. Specifically, the Gram matrix $\mathcal{G}_{|\phi\rangle}$ is full rank if and only if*

$$b_0 b_1 \neq 0 \quad \text{and} \quad \theta \notin \left\{0, \frac{\pi}{2}, \pi, \frac{3\pi}{2}\right\},$$

for fiducial states of the form $|\phi\rangle = b_0|0\rangle + b_1 e^{i\theta}|1\rangle$. This provides a necessary and sufficient condition, and defines a continuous family of IC fiducials that vastly enlarges the space compared to the two known SIC-POVM fiducials in dimension two.

Complete proofs of Theorem 2 and the $d = 2$ characterization are given in Appendix C.

Theorem 3 (Fiducial states that fail to achieve informational completeness). *Let $|\phi\rangle \in \mathbb{C}^d$ be a pure state, and let $\mathcal{G}_{|\phi\rangle}$ denote the Gram matrix formed from the Weyl–Heisenberg orbit $\{M_\alpha|\phi\rangle\}$. Then $\mathcal{G}_{|\phi\rangle}$ is rank-deficient—and thus the corresponding POVM is not informationally complete—if $|\phi\rangle$ satisfies any of the following conditions:*

1. $|\phi\rangle$ is real-valued (i.e., all components $a_j \in \mathbb{R}$) when the dimension d is even.
2. $|\phi\rangle = \frac{1}{\sqrt{d}} \sum_k a_k |k\rangle$ with each coefficient a_k a root of unity (i.e., $a_k^{m_k} = 1$ for some $m_k \in \mathbb{Z}^+$).
3. $|\phi\rangle$ is sparse, with at most $k \leq \sqrt{d - \frac{3}{4}} + \frac{1}{2}$ nonzero components.
4. $|\phi\rangle$ is a qudit stabilizer state.

In each case, the Gram matrix $\mathcal{G}_{|\phi\rangle}$ is not of full rank, and hence the associated Weyl–Heisenberg orbit fails to yield an IC-POVM.

A detailed proof is provided in Appendix D. Furthermore, in the n -qubit setting, we identify certain quantum circuits U for which the output state $|\phi\rangle = U|0\rangle^{\otimes n}$ fails to generate an IC-POVM.

Theorem 4 (Representation of arbitrary quantum states via minimal IC-POVMs by Weyl–Heisenberg orbits). *Let $\{|\phi_\alpha\rangle\}_{\alpha=0}^{d^2-1}$ be the Weyl–Heisenberg orbit of a fiducial state $|\phi\rangle$, forming a minimal IC-POVM by normalization. For an unknown quantum state ρ , define the measurement probabilities*

$$p_\alpha = \text{tr}(\rho |\phi_\alpha\rangle\langle\phi_\alpha|). \quad (15)$$

Let $\mathcal{G}_{|\phi\rangle} = \sum_{m,n} \lambda_{mn} |\Phi_{mn}\rangle\langle\Phi_{mn}|$ be the spectral decomposition of the corresponding Gram matrix, with eigenvalues λ_{mn} and eigenvectors $|\Phi_{mn}\rangle$. Then density operator ρ admits the following exact reconstruction:

$$\rho = \sum_{\alpha=0}^{d^2-1} \left(\sum_{m,n=0}^{d-1} \lambda_{mn}^{-1} \langle\Phi_{mn}|\mathbf{p}\rangle \langle\alpha|\Phi_{mn}\rangle \right) |\phi_\alpha\rangle\langle\phi_\alpha| \quad (16)$$

where $\mathbf{p} = (p_0, \dots, p_{d^2-1})^T$ is the vector of measurement outcomes.

A detailed proof is provided in Appendix E.

Theorem 5 (Qudit classical shadow tomography using IC-POVMs from Weyl–Heisenberg orbits). *Let $\{|\phi_k\rangle\}_{k=0}^{d^2-1}$ be a minimal IC-POVM formed from the Weyl–Heisenberg orbit of a fiducial state $|\phi\rangle$, and let \mathcal{G} be its associated Gram matrix.*

When an unknown quantum state ρ is measured and outcome k is observed, the corresponding classical shadow estimator in a single measurement is given by

$$F^{-1}(|\phi_k\rangle\langle\phi_k|) = d \sum_{\alpha=0}^{d^2-1} \mathcal{G}_{\alpha k}^{-1} |\phi_\alpha\rangle\langle\phi_\alpha|, \quad (17)$$

where \mathcal{G}^{-1} is the inverse of Gram matrix.

To estimate the expectation value $\text{tr}(\rho O)$ for an observable O , define the traceless component $O_0 = O - \text{tr}(O)/d$. Then, the shadow norm for the variance is bounded by

$$\|O_0\|_{\text{shadow}}^2 \leq \frac{d}{\lambda_{\min}} \text{tr}(O_0^2), \quad (18)$$

where λ_{\min} denotes the smallest eigenvalue of the Gram matrix \mathcal{G} .

Moreover, when the state ρ is drawn randomly from the Haar measure, the average-case variance is bounded as

$$\|O_0\|_{\text{average}}^2 \leq \frac{1}{\lambda_{\min}} \text{tr}(O_0^2). \quad (19)$$

A detailed proof is provided in Appendix F.

Remark 2. When the observable O to be predicted admits a known decomposition over the Weyl–Heisenberg orbit, i.e.,

$$O = \sum_{k=0}^{d^2-1} c_k |\phi_k\rangle\langle\phi_k|,$$

then the classical shadow post-processing becomes extremely efficient. Specifically, the estimator satisfies

$$\text{tr}(F^{-1}(|\phi_k\rangle\langle\phi_k|) \cdot O) = d \cdot c_k,$$

meaning that the contribution of each measurement outcome can be computed in constant time once the coefficients c_k are known.

Moreover, these coefficients can be reconstructed from the spectral data of the Gram matrix via Eq. (16),

$$c_k = \sum_{m,n=0}^{d-1} \lambda_{mn}^{-1} \langle\Phi_{mn}|\mathbf{o}\rangle\langle k|\Phi_{mn}\rangle,$$

where $\mathbf{o} \in \mathbb{R}^{d^2}$ is the vector with components $o_\alpha = \text{tr}(O|\phi_\alpha\rangle\langle\phi_\alpha|)$.

Property 2 (Range of the minimum eigenvalue of the Gram matrix). Let $\mathcal{G}_{|\phi\rangle} \in \mathbb{C}^{d^2 \times d^2}$ be the Gram matrix associated with the Weyl–Heisenberg orbit of a normalized fiducial state $|\phi\rangle \in \mathbb{C}^d$. Then, the minimum eigenvalue of $\mathcal{G}_{|\phi\rangle}$, denoted by λ_{\min} , satisfies

$$0 \leq \lambda_{\min} \leq \frac{d}{d+1}.$$

If the orbit forms a SIC-POVM, the upper bound is achieved.

A detailed derivation is provided in Appendix G.

Property 3 (Spectrum of the Gram matrix for SIC-POVM). If the fiducial state $|\phi\rangle$ generates a SIC-POVM through its Weyl–Heisenberg orbit, the Gram matrix takes the symmetric form

$$\mathcal{G}_{|\phi\rangle} = \frac{1}{d+1} \begin{pmatrix} d+1 & 1 & \cdots & 1 \\ 1 & d+1 & \cdots & 1 \\ \vdots & \vdots & \ddots & \vdots \\ 1 & 1 & \cdots & d+1 \end{pmatrix}. \quad (20)$$

The eigenvalues of $\mathcal{G}_{|\phi\rangle} \in \mathbb{C}^{d^2 \times d^2}$ are:

- one eigenvalue equal to d ,
- $d^2 - 1$ eigenvalues equal to $\frac{d}{d+1}$.

A detailed derivation is provided in Appendix H. Therefore, the minimal eigenvalue is

$$\lambda_{\min:\text{SIC}} = \frac{d}{d+1}.$$

Substituting this into the worst-case variance bound of classical shadow tomography gives

$$\|O_0\|_{\text{shadow}}^2 \leq \frac{d}{\lambda_{\min}} \text{tr}(O_0^2) = (d+1) \text{tr}(O_0^2),$$

which matches the performance guarantee for classical shadows using random MUBs.

IV. NUMERICAL ANALYSIS

To complement our theoretical results, we perform numerical simulations to examine the behavior of Gram matrices associated with random fiducial states and assess their potential to generate informationally complete POVMs (IC-POVMs).

Determinant Instability in High Dimensions. Although the determinant of the Gram matrix provides a sufficient condition for informational completeness, it becomes numerically unstable in high dimensions due to rapid decay. This makes it unreliable as a practical criterion in large systems.

To illustrate this, we sample 1000 Haar-random pure states $|\phi\rangle$ for each dimension $d \in \{4, \dots, 50\}$, compute their associated Gram matrices, and record the mean determinant values. As shown in Fig. 1, the determinant decreases exponentially with increasing d , falling below machine precision (e.g., 10^{-320}) for $d \geq 40$. This motivates the use of the minimum eigenvalue as a more robust alternative.

Minimum Eigenvalue Distribution. Instead of relying on the determinant, we study the smallest eigenvalue λ_{\min} of the Gram matrix, which directly indicates whether the matrix is full rank. According to Theorem 2, our explicit constructions yield Gram matrices with provably positive minimum eigenvalues.

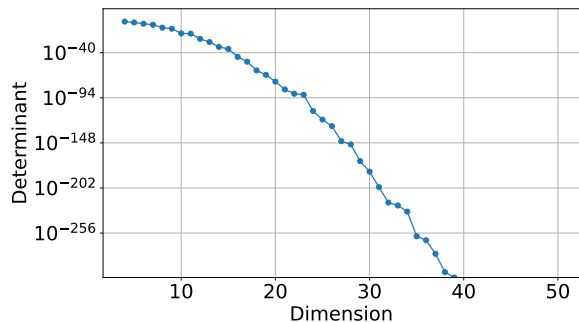


FIG. 1: Mean determinants of Gram matrices for 1000 Haar-random fiducial states across dimensions $d = 4$ to 50.

Figure 2 shows the empirical mean and standard deviation of the minimum eigenvalue λ_{\min} across 1000 Haar-random fiducial states for each dimension. The blue curve represents the sample mean, the shaded region indicates the standard deviation, and the red curve denotes the theoretical lower bound obtained from our explicit construction in Theorem 2.

Remarkably, the empirical means consistently lie above the theoretical lower bound, particularly in higher dimensions. This indicates that Haar-random fiducial states are, on average, more likely to generate full-rank Gram matrices than our deterministic constructions. In other words, in high-dimensional settings, a randomly chosen fiducial state has a high probability of yielding an IC-POVM via the Weyl–Heisenberg orbit.

Interestingly, the global plot reveals apparent irregularities: the sequence of mean values exhibits discontinuities between even and odd dimensions. However, when the data is separated by parity, as shown in Figs. 3, each subsequence becomes smooth and monotonic. This suggests that the spectral behavior of Gram matrices may be influenced by structural differences tied to the parity of d , potentially related to underlying group-theoretic properties of the Weyl–Heisenberg orbit.

Quantum State Tomography Using IC-POVMs from Weyl–Heisenberg Orbits. We now evaluate the effectiveness of using IC-POVMs constructed from Weyl–Heisenberg orbits for quantum state tomography. Given a fiducial state $|\phi\rangle$ such that the associated Gram matrix is full rank (i.e., $\lambda_{\min} > 0$), we obtain a set of d^2 rank-one projectors $\{|\phi_k\rangle\langle\phi_k|\}$ through Weyl–Heisenberg group action. These form an IC-POVM by normalization that can be used to reconstruct an unknown quantum state ρ .

Using the Born rule, we simulate M measurements on ρ , where the frequency of outcome k approximates $q_k \approx \text{tr}(\rho E_k)$, with $E_k = |\phi_k\rangle\langle\phi_k|/d$. Based on the measured probabilities $\{q_k\}$, we employ two reconstruction methods:

1. **Linear Inversion.** Using the explicit decomposi-

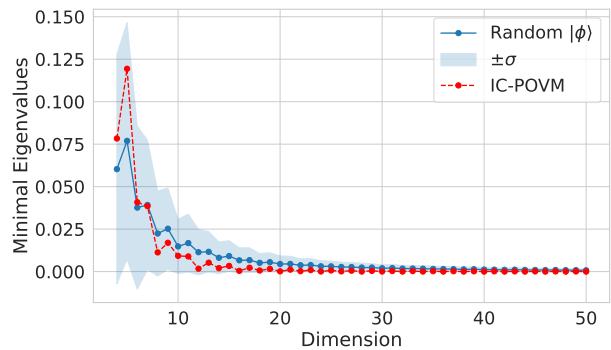
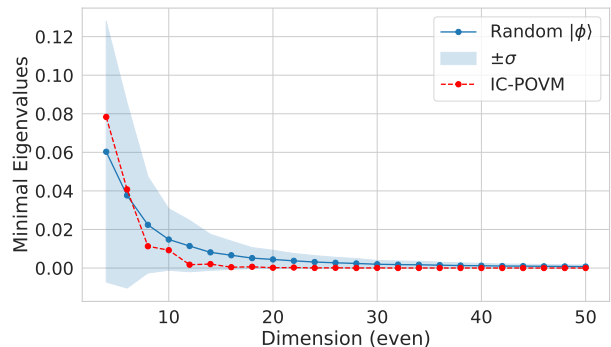
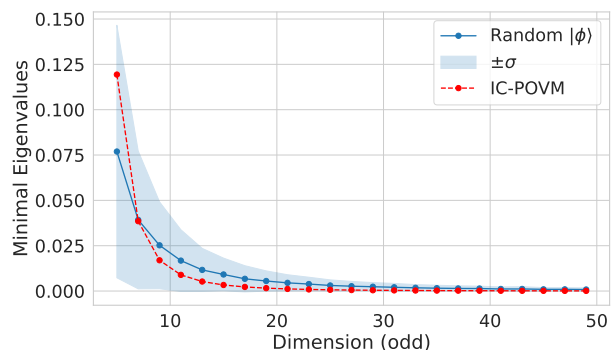


FIG. 2: Mean and standard deviation of the minimum eigenvalues λ_{\min} of Gram matrices for 1000 Haar-random fiducial states, over dimensions $d = 4$ to 50. The blue line shows the empirical mean, the shaded region indicates the standard deviation, and the red line marks the theoretical lower bound from Theorem 2.



(a) Minimum eigenvalues λ_{\min} for Haar-random fiducial states in even dimensions.



(b) Minimum eigenvalues λ_{\min} for Haar-random fiducial states in odd dimensions.

FIG. 3: Comparison of λ_{\min} trends for Haar-random fiducial states across even and odd dimensions ($d = 4$ to 50). While both exhibit smooth decay, subtle differences in spectral behavior emerge due to dimensional parity.

tion formula derived in Eq. (16), which expresses ρ as a linear combination of projectors $|\phi_k\rangle\langle\phi_k|$, weighted by coefficients computed via the Gram matrix spectrum.

2. Convex Optimization (SDP). Solving the following least-squares semidefinite program:

$$\hat{X} = \arg \min_X \sum_{k=0}^{d^2-1} |\text{tr}(X|\phi_k\rangle\langle\phi_k|) - q_k|^2, \quad (21)$$

subject to $X \succeq 0, \quad \text{tr}(X) = 1.$

To evaluate performance, we randomly sample 100 Haar-random pure states ρ and compute the average fidelity between the true and reconstructed states as a function of the total number of measurements M . The blue curves correspond to the linear inversion method using Eq. (16), while the red curves show the results of the SDP-based approach.

Figure 4 illustrate the average fidelity performance for dimensions $d = 4, 8, 16, 32$, respectively. In all cases, both methods converge toward high-fidelity reconstructions as the number of measurements increases. The SDP-based approach exhibits better performance in the low-sample regime due to its physicality constraints. However, when the number of measurements becomes sufficiently large, the linear estimator based on Eq. (16) slightly surpasses the SDP method in fidelity, owing to its unbiased nature and analytical structure.

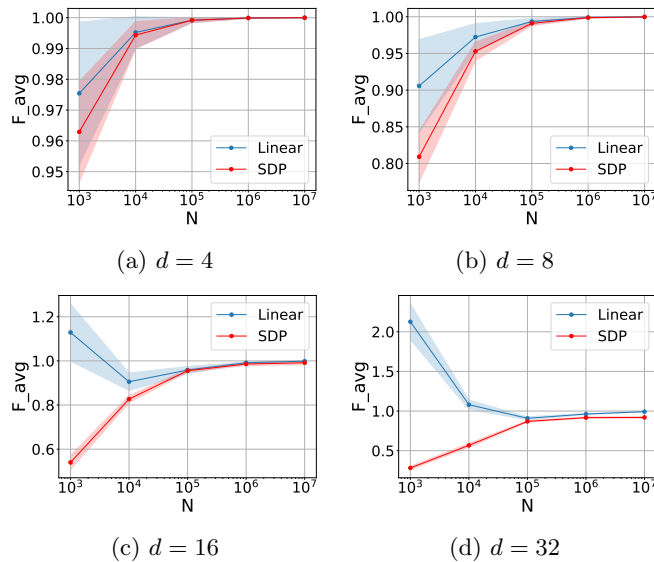


FIG. 4: Average fidelity versus the number of measurements for quantum state tomography using IC-POVMs.

Visualizing Gram Matrix Structure and Spectral Properties. To visualize and compare the spectral and structural properties of different fiducial states under Weyl–Heisenberg orbits, we generate composite plots that include:

- the heatmap of the Gram matrix $\mathcal{G}_{|\phi\rangle}$,
- the corresponding eigenvalue magnitude matrix (reordered into 2D form), and
- a histogram of the eigenvalue distribution.

These visualizations reveal global symmetries, spectral concentration, and the presence or absence of small eigenvalues, which are crucial for assessing informational completeness and numerical stability in state reconstruction.

From these visualizations, we observe that the Gram matrix $\mathcal{G}_{|\phi\rangle}$ exhibits a form of cyclic symmetry: the matrix is invariant under simultaneous shifts of rows and columns, which corresponds to the translation symmetry of the underlying Weyl–Heisenberg group. As implied by Eq. (8), the sum of each row or column is exactly d , and consequently the largest eigenvalue of $\mathcal{G}_{|\phi\rangle}$ is always d . Moreover, the trace of the Gram matrix equals d^2 , implying that the sum of all eigenvalues is also d^2 .

Among the examples shown, the SIC-POVM configuration exhibits the most uniform eigenvalue distribution, consistent with its highly symmetric construction and optimal frame properties. This uniformity contributes to better numerical conditioning and lower variance in applications of qudit classical shadow tomography.

Optimizing fiducial states for improved shadow performance. In classical shadow tomography, the sample complexity is inversely proportional to the minimum eigenvalue λ_{\min} of the Gram matrix. As shown in Fig. 2, when fiducial states are chosen at random, λ_{\min} typically decreases rapidly as the dimension d increases, leading to significantly higher sampling costs in high-dimensional systems.

To mitigate this effect, we formulate the following optimization problem: for a given dimension d , we seek a normalized fiducial state $|\phi\rangle \in \mathbb{C}^d$ that maximizes the minimum eigenvalue of its associated Gram matrix $\mathcal{G}_{|\phi\rangle}$, defined over the Weyl–Heisenberg orbit. Formally,

$$\max_{|\phi\rangle \in \mathbb{C}^d} \lambda_{\min}(\mathcal{G}_{|\phi\rangle}) = \max_{|\phi\rangle \in \mathbb{C}^d} \min\{\lambda_{mn}\}_{m,n}$$

subject to $\langle\phi|\phi\rangle = 1.$

Here, the eigenvalues λ_{mn} are given explicitly by the 2D discrete Fourier transform in Eq. (12), allowing efficient computation.

Since the objective is highly non-convex, we adopt large-scale gradient-based optimization using the Adam optimizer, combined with extensive random restarts to escape poor local minima. For each dimension $d \in \{2, \dots, 20\}$, we run 2500 optimization steps with a learning rate of 0.05, repeated over 3000 random initializations. The best-performing result for each dimension is recorded.

As shown in Fig. 7, the optimized values of λ_{\min} significantly improve over random baselines. Remarkably, in low dimensions, these values approach the theoretical upper bound $\frac{d}{d+1}$, corresponding to the ideal performance of SIC-POVMs. Although our resulting orbits do

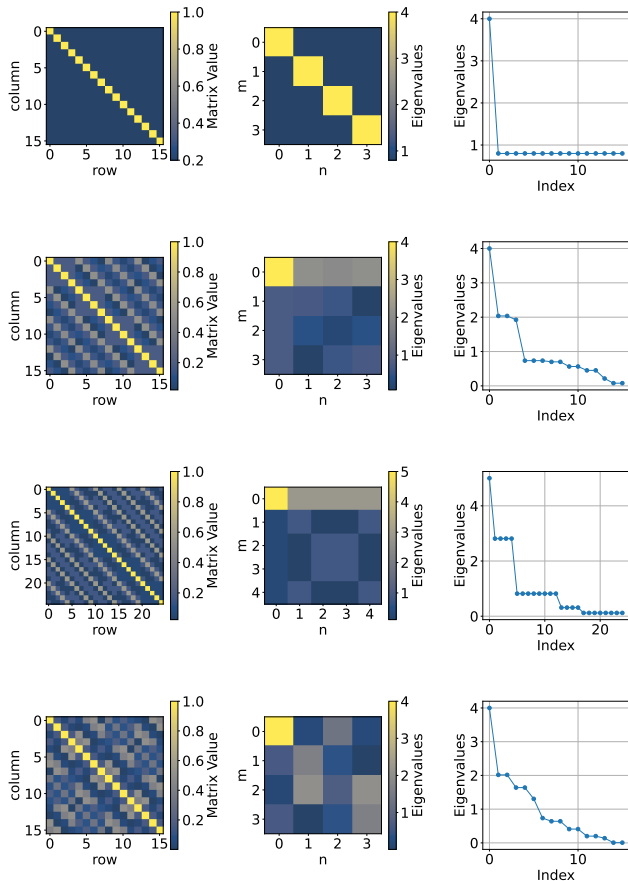


FIG. 5: Composite visualizations of the Gram matrix structure and spectral properties for different fiducial states. Each row shows, from left to right: the Gram matrix heatmap, the 2D DFT-arranged eigenvalue matrix, and the histogram of eigenvalue distribution. (a) SIC-POVM in $d = 4$, exhibiting the most uniform eigenvalue distribution; (b) IC-POVM in $d = 4$ with fiducial state in Eq. (13); (c) IC-POVM in dimension $d = 5$ in Eq. (14); (d) Haar-random fiducial state in $d = 4$, with less structured spectrum and broader eigenvalue spread.

not form SIC-POVMs, they nonetheless yield comparable sampling efficiency in classical shadow tomography.

Compared to the standard approach of constructing SIC-POVMs—which requires minimizing the fourth-moment functional to saturate Welch’s bound [Ref]—our method is substantially simpler and more flexible. Intuitively, SIC-POVM construction seeks fiducial states whose Gram spectra are exactly $\{d, \frac{d}{d+1}, \dots, \frac{d}{d+1}\}$, enforcing global symmetry across all eigenvalues. In contrast, our optimization only requires $\lambda_{\min} = \Omega(1)$ to ensure efficient shadow reconstruction. This weaker requirement translates to a more tractable numerical problem with fewer structural constraints.

Moreover, because the eigenvalues are analytically connected to the fiducial state via a 2D discrete Fourier

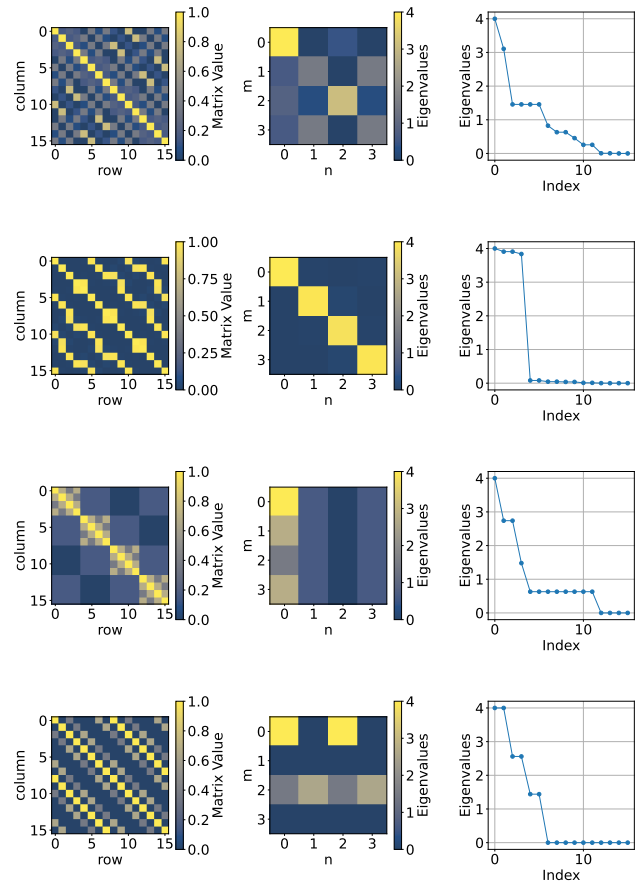


FIG. 6: Composite visualizations of the Gram matrix structure and spectral properties for different fiducial states. Each row shows, from left to right: the Gram matrix heatmap, the 2D DFT-arranged eigenvalue matrix, and the histogram of eigenvalue distribution.

(a) non-IC-POVM in $d = 4$ with real-valued components; (b) non-IC-POVM in $d = 4$ with roots of unity components; (c) non-IC-POVM in $d = 4$ with 2 zero components; (d) qudit stabilizer state in $d = 4$ with $\phi = \frac{1}{\sqrt{10}}(1, 2i, 1, 2i)$.

transform, our objective remains differentiable and scalable. This enables standard optimization tools to be effectively applied even in high-dimensional settings. Hence, our approach achieves near-optimal shadow performance with significantly lower computational and structural overhead compared to exact SIC-POVM constructions.

Acknowledgements— This work received support from the National Natural Science Foundation of China through Grants No. 62001260 and No. 42330707, and from the Beijing Natural Science Foundation under Grant No. Z220002.

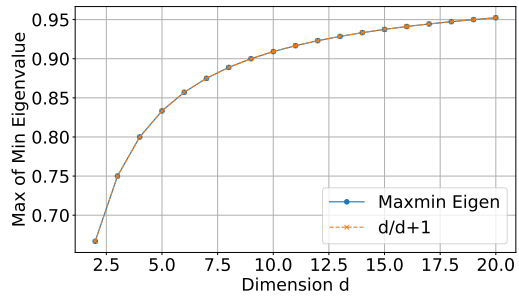


FIG. 7: Optimal Maximal minimal eigenvalues

Appendix A: Proof of Proposition 1: Tight frame of Weyl-Heisenberg orbit

Proof. We compute the operator sum:

$$S := \sum_{j,k=0}^{d-1} X^j Z^k |\phi\rangle \langle \phi| Z^{-k} X^{-j}.$$

Fixing j , consider the inner sum over k :

$$S_j := \sum_{k=0}^{d-1} Z^k |\phi\rangle \langle \phi| Z^{-k}.$$

Let $|\phi\rangle = \sum_{a=0}^{d-1} a_a |a\rangle$. Then:

$$Z^k |\phi\rangle = \sum_{a=0}^{d-1} \omega^{ak} a_a |a\rangle, \quad \text{where } \omega = e^{2\pi i/d}.$$

Thus:

$$Z^k |\phi\rangle \langle \phi| Z^{-k} = \sum_{a,b} \omega^{k(a-b)} a_a a_b^* |a\rangle \langle b|,$$

and summing over k , we get:

$$S_j = \sum_{a,b} \left(\sum_{k=0}^{d-1} \omega^{k(a-b)} \right) a_a a_b^* |a\rangle \langle b|.$$

Because:

$$\sum_{k=0}^{d-1} \omega^{k(a-b)} = \begin{cases} d, & \text{if } a = b, \\ 0, & \text{otherwise,} \end{cases}$$

it follows that:

$$S_j = d \sum_{a=0}^{d-1} |a_a|^2 |a\rangle \langle a|,$$

which is a diagonal matrix with entries proportional to the probabilities $|a_a|^2$.

Now, summing over j and applying the shift operators X^j :

$$S = \sum_{j=0}^{d-1} X^j S_0 X^{-j}.$$

Since each X^j cyclically permutes the diagonal entries of S_0 , the full sum S uniformly distributes the diagonal weights. Therefore:

$$S = d \cdot I,$$

completing the proof. □

Appendix B: Proof of Theorem 1: Diagonalization of the Gram Matrix

In this section, we derive the expression for the eigenvalues of the Gram matrix $\mathcal{G}_{|\phi\rangle}$ associated with the Weyl-Heisenberg orbit of a fiducial state $|\phi\rangle$. Recall that the Gram matrix is defined by the inner products between all orbit elements $X^j Z^k |\phi\rangle$, and its matrix elements are given by

$$\mathcal{G}_{(j,k),(j',k')} = \langle \phi| Z^{-k} X^{-j} X^{j'} Z^{k'} |\phi\rangle = \langle \phi| X^{j'-j} Z^{k'-k} |\phi\rangle.$$

As such, $\mathcal{G}_{|\phi\rangle}$ is a $d^2 \times d^2$ circulant matrix on a two-dimensional discrete torus. It follows from standard harmonic analysis that its eigenvectors are tensor products of Fourier basis vectors, and its eigenvalues are given by the two-dimensional discrete Fourier transform (2D DFT) of the matrix: $P_{jk} = |\langle\phi|X^j Z^k|\phi\rangle|^2$. Next, we give an detailed proof.

Proof. We aim to prove that

$$\mathcal{G}_{|\phi\rangle}|\Phi_{mn}\rangle = \mathcal{G}_{|\phi\rangle}|\mathcal{F}_m\rangle \otimes |\mathcal{F}_n\rangle = \lambda_{mn}|\mathcal{F}_m\rangle \otimes |\mathcal{F}_n\rangle, \quad (\text{B1})$$

for all $m, n \in \{0, 1, \dots, d-1\}$.

We first express

$$|\mathcal{F}_m\rangle \otimes |\mathcal{F}_n\rangle = \frac{1}{d} \sum_{s=0}^{d-1} \sum_{t=0}^{d-1} a_{st}|s\rangle|t\rangle. \quad (\text{B2})$$

Namely, a_{st} denotes the coefficient of the basis state $|s\rangle|t\rangle$ in the expansion of $|\mathcal{F}_m\rangle \otimes |\mathcal{F}_n\rangle$, up to factor $1/d$.

Since $|\mathcal{F}_m\rangle = \frac{1}{\sqrt{d}} \sum_{s=0}^{d-1} \omega^{sm}|s\rangle$, we obtain

$$|\mathcal{F}_m\rangle \otimes |\mathcal{F}_n\rangle = \frac{1}{d} \sum_{s=0}^{d-1} \sum_{t=0}^{d-1} \omega^{ms+nt}|s\rangle|t\rangle,$$

and thus

$$a_{st} = \omega^{ms+nt}. \quad (\text{B3})$$

We now aim to prove

$$\langle j| \otimes \langle k| \mathcal{G}_{|\phi\rangle} |\mathcal{F}_m\rangle \otimes |\mathcal{F}_n\rangle = \lambda_{mn} \frac{1}{d} a_{jk} = \frac{1}{d} \lambda_{mn} \omega^{mj+nk}, \quad (\text{B4})$$

for all j, k .

As $\mathcal{G}_{|\phi\rangle}$ is Hermitian, we have $\mathcal{G}_{|\phi\rangle}^\dagger = \mathcal{G}_{|\phi\rangle}$. To compute the inner product $\langle j| \otimes \langle k| \mathcal{G}_{|\phi\rangle} |\mathcal{F}_m\rangle \otimes |\mathcal{F}_n\rangle$, we first simplify $\mathcal{G}_{|\phi\rangle}|j\rangle \otimes |k\rangle$.

By Eq. (7), we have

$$\mathcal{G}_{|\phi\rangle}|j\rangle \otimes |k\rangle = \sum_{m_1=0}^{d-1} \sum_{n_1=0}^{d-1} |\langle\phi|(X^{m_1} Z^{n_1})^\dagger(X^j Z^k)|\phi\rangle|^2 \cdot |m_1 n_1\rangle. \quad (\text{B5})$$

We now calculate the inner product between the vectors in Eq. (B5) and Eq. (11):

$$\begin{aligned} \langle j| \otimes \langle k| \mathcal{G}_{|\phi\rangle} |\mathcal{F}_m\rangle \otimes |\mathcal{F}_n\rangle &= \sum_{m_1=0}^{d-1} \sum_{n_1=0}^{d-1} |\langle\phi|(X^{m_1} Z^{n_1})^\dagger(X^j Z^k)|\phi\rangle|^2 \cdot \langle m_1 n_1| \cdot \frac{1}{d} \sum_{s=0}^{d-1} \sum_{t=0}^{d-1} \omega^{ms+nt}|s\rangle|t\rangle \\ &= \frac{1}{d} \sum_{m_1=0}^{d-1} \sum_{n_1=0}^{d-1} |\langle\phi|(X^{m_1} Z^{n_1})^\dagger(X^j Z^k)|\phi\rangle|^2 \cdot \omega^{mm_1+nn_1} \\ &= \frac{1}{d} \sum_{m_1=0}^{d-1} \sum_{n_1=0}^{d-1} |\langle\phi|X^{m_1-j} Z^{n_1-k}|\phi\rangle|^2 \cdot \omega^{mm_1+nn_1} \\ &= \frac{1}{d} \sum_{m_1=0}^{d-1} \sum_{n_1=0}^{d-1} |\langle\phi|X^{m_1-j} Z^{n_1-k}|\phi\rangle|^2 \cdot \omega^{m(m_1-j)+n(n_1-k)} \omega^{mj+nk} \\ &= \frac{1}{d} \left[\sum_{m_1=0}^{d-1} \sum_{n_1=0}^{d-1} |\langle\phi|X^{m_1} Z^{n_1}|\phi\rangle|^2 \cdot \omega^{mm_1+nn_1} \right] \omega^{mj+nk} \end{aligned} \quad (\text{B6})$$

Thus, we define

$$\lambda_{mn} := \sum_{m_1=0}^{d-1} \sum_{n_1=0}^{d-1} |\langle\phi|X^{m_1} Z^{n_1}|\phi\rangle|^2 \cdot \omega^{mm_1+nn_1}. \quad (\text{B7})$$

We have therefore shown that each of the d^2 tensor-product vectors $|\mathcal{F}_m\rangle \otimes |\mathcal{F}_n\rangle$, constructed from the Fourier basis, is an eigenvector of the Gram matrix $\mathcal{G}_{|\phi\rangle}$, with corresponding eigenvalue λ_{mn} . \square

Lemma 1. All eigenvalues λ_{mn} of the Gram matrix in Eq. (7) can be expressed as in Eq. (B11).

Proof. For any state $|\phi\rangle = \sum_{k=0}^{d-1} a_k |k\rangle$, we have

$$Z^{n_1} |\phi\rangle = \sum_{k=0}^{d-1} \omega^{n_1 k} a_k |k\rangle \quad (\text{B8})$$

and

$$X^{-m_1} |\phi\rangle = \sum_{k=0}^{d-1} a_k |k - m_1 \bmod d\rangle = \sum_{k=0}^{d-1} a_{k+m_1 \bmod d} |k\rangle \quad (\text{B9})$$

Thus we have

$$\begin{aligned} |\langle \phi | X^{m_1} Z^{n_1} | \phi \rangle|^2 &= \left| \left(\sum_{k=0}^{d-1} a_{k+m_1 \bmod d}^* \langle k | \right) \sum_{j=0}^{d-1} \omega^{n_1 j} a_j |j\rangle \right|^2 \\ &= \left| \sum_{k=0}^{d-1} a_k a_{k+m_1 \bmod d}^* \cdot \omega^{n_1 k} \right|^2 \end{aligned} \quad (\text{B10})$$

From now on, we omit the notation $\bmod d$ in the index of coefficients for simplicity.

Then the eigenvalue λ_{mn} can be expressed as:

$$\lambda_{mn} = \sum_{m_1=0}^{d-1} \sum_{n_1=0}^{d-1} \omega^{m_1 m + n_1 n} \left| \sum_{k=0}^{d-1} a_k a_{k+m_1}^* \omega^{n_1 k} \right|^2 \quad (\text{B11})$$

□

Appendix C: Proof of Theorem 2: Existence of Informationally Complete Fiducial States for Arbitrary Dimension

1. Full Rank Criterion for $d = 2$

Statement 1. We consider the fiducial state of the form

$$|\phi\rangle = b_0 |0\rangle + b_1 e^{i\theta} |1\rangle.$$

Here we prove that the Gram matrix $\mathcal{G}_{|\phi\rangle}$ is full rank if and only if

$$b_0 b_1 \neq 0 \quad \text{and} \quad \theta \notin \{0, \pi/2, \pi, 3\pi/2\}. \quad (\text{C1})$$

Proof. When $d = 2$, the root of unity is $\omega = -1$. From Eq. (B11), we compute

$$\begin{aligned} \lambda_{mn} &= \sum_{m_1=0}^1 \sum_{n_1=0}^1 (-1)^{m_1 m + n_1 n} |a_{m_1}^* a_0 + a_{1+m_1}^* a_1 (-1)^{n_1}|^2 \\ &= \sum_{n_1=0}^1 (-1)^{n_1 n} \left(|a_0|^2 + |a_1|^2 (-1)^{n_1} \right)^2 + (-1)^m |a_1^* a_0 + a_0^* a_1 (-1)^{n_1}|^2 \\ &= |a_0|^2 + |a_1|^2 + (-1)^n (|a_0|^2 - |a_1|^2)^2 + (-1)^m |a_1^* a_0 + a_0^* a_1|^2 + (-1)^{m+n} |a_1^* a_0 - a_0^* a_1|^2 \\ &= (1 + (-1)^n) (|a_0|^4 + |a_1|^4) + (1 - (-1)^n) 2|a_0 a_1|^2 \\ &\quad + (-1)^m (1 + (-1)^n) 2|a_0 a_1|^2 + (-1)^m (1 - (-1)^n) (a_0^{*2} a_1^2 + a_0^2 a_1^{*2}) \end{aligned} \quad (\text{C2})$$

This leads to the following expressions:

$$\lambda_{m,0} = 2 (|a_0|^2 + (-1)^m |a_1|^2)^2 = 2 (b_0^2 + (-1)^m b_1^2 e^{2i\theta})^2, \quad (\text{C3})$$

$$\lambda_{m,1} = 2 (-1)^m b_0^2 b_1^2 (e^{i\theta} + (-1)^m e^{-i\theta})^2. \quad (\text{C4})$$

Hence, $\det(\mathcal{G}_{|\phi\rangle}) \neq 0$ if and only if the following four expressions are not all zero:

$$b_0^2 + b_1^2 e^{2i\theta}, \quad b_0^2 - b_1^2 e^{2i\theta}, \quad b_0 b_1 (e^{i\theta} + e^{-i\theta}), \quad b_0 b_1 (e^{i\theta} - e^{-i\theta}).$$

Note that the conditions $b_0 b_1 (e^{i\theta} + e^{-i\theta}) \neq 0$ and $b_0 b_1 (e^{i\theta} - e^{-i\theta}) \neq 0$ directly lead to the constraint in Eq. (C1). When either of these is violated, the quantity $e^{2i\theta}$ becomes non-real, and thus the other two expressions cannot simultaneously vanish. Therefore, the constraint in Eq. (C1) is sufficient to ensure that $\mathcal{G}_{|\phi\rangle}$ is full rank, and the resulting Weyl–Heisenberg orbit forms an IC-POVM. \square

It is well known that for $d = 2$, there exist exactly two fiducial states (up to global phase and Weyl–Heisenberg equivalence) that generate a SIC-POVM. These are given by

$$\left\{ \frac{1}{\sqrt{6}} \left(\sqrt{3 + \sqrt{3}}, e^{\pi i/4} \sqrt{3 - \sqrt{3}} \right), \quad \frac{1}{\sqrt{6}} \left(-\sqrt{3 - \sqrt{3}}, e^{\pi i/4} \sqrt{3 + \sqrt{3}} \right) \right\}.$$

In this work, we extend the analysis by relaxing the symmetry constraint required for SIC-POVMs and instead explore the broader class of fiducial states that yield IC-POVMs through their Weyl–Heisenberg orbits. This generalization admits more flexible configurations beyond the regular tetrahedral symmetry and paves the way for systematic investigation in higher dimensions.

2. IC Fiducial Construction for Even Dimensions

We analyze the fiducial state $|\phi\rangle = |0\rangle + \sum_{j=1}^{d-1} \zeta^j |j\rangle$, and show that all the eigenvalues $\{\lambda_{mn}\}$ are nonzero for even dimensions.

Statement 2. *Let d be an even positive integer, and let $\zeta = e^{2\pi i/(d+1)}$ be a primitive $(d+1)$ -th root of unity. Consider the unnormalized fiducial state*

$$|\phi\rangle = |0\rangle + \sum_{t=0}^{d-1} \zeta^t |t\rangle.$$

Then the corresponding Gram matrix $\mathcal{G}_{|\phi\rangle}$ formed from the Weyl–Heisenberg orbit of $|\phi\rangle$ is full rank and hence the orbit generates an IC-POVM. Moreover, all d^2 eigenvalues λ_{mn} of $\mathcal{G}_{|\phi\rangle}$ are strictly positive.

Proof. We define the Kronecker delta function as

$$\delta_{j,k} = \begin{cases} 1, & \text{if } j = k, \\ 0, & \text{otherwise.} \end{cases}$$

The coefficient a_t of the state $|\phi\rangle$ can thus be expressed as $a_t = (\delta_{t,0} + 1)\zeta^t$, accounting for the special role of $|0\rangle$ in the unnormalized superposition.

We should notice that,

$$a_{t+m_1} = \begin{cases} (\delta_{t+m_1,0} + 1)\zeta^{t+m_1}, & \text{if } 0 \leq t \leq d-1-m_1, \\ (\delta_{t+m_1-d,0} + 1)\zeta^{t+m_1-d}, & \text{if } d-m_1 \leq t \leq d-1. \end{cases} \quad (\text{C5})$$

Here, the influence of modulo- d arithmetic is taken into consideration to reflect explicit calculations.

Take the Eq. (C5) into the eigenvalue expression of Eq. (B11), we have

$$\begin{aligned}
& \lambda_{mn} \\
&= \sum_{m_1, n_1} \omega^{m_1 m + n_1 n} \left| \sum_t a_{t+m_1}^* a_t \omega^{tn_1} \right|^2 \\
&= \sum_{m_1, n_1} \omega^{m_1 m + n_1 n} \left| \sum_{t=0}^{d-1-m_1} (\delta_{t+m_1,0} + 1) \zeta^{-t-m_1} (\delta_{t,0} + 1) \zeta^t \omega^{tn_1} + \sum_{t=d-m_1}^{d-1} (\delta_{t+m_1-d,0} + 1) \zeta^{d-m_1} \omega^{tn_1} \right|^2 \\
&= \sum_{m_1, n_1} \omega^{m_1 m + n_1 n} \left| \sum_{t=0}^{d-1-m_1} (\delta_{t+m_1,0} + 1) (\delta_{t,0} + 1) \omega^{tn_1} + \sum_{t=d-m_1}^{d-1} (\delta_{t+m_1-d,0} + 1) \zeta^d \omega^{tn_1} \right|^2 \cdot |\zeta^{-m_1}|^2 \\
&= \sum_{m_1, n_1} \omega^{m_1 m + n_1 n} \left(\sum_{t=0}^{d-1-m_1} (\delta_{t+m_1,0} + 1) (\delta_{t,0} + 1) \omega^{tn_1} + \sum_{t=d-m_1}^{d-1} (\delta_{t+m_1-d,0} + 1) \zeta^d \omega^{tn_1} \right) \\
&\quad \cdot \left(\sum_{s=0}^{d-1-m_1} (\delta_{s+m_1,0} + 1) (\delta_{s,0} + 1) \omega^{-sn_1} + \sum_{s=d-m_1}^{d-1} (\delta_{s+m_1-d,0} + 1) \zeta^{-d} \omega^{-sn_1} \right) \\
&= \sum_{m_1, n_1} \omega^{m_1 m + n_1 n} \sum_{0 \leq t, s \leq d-1-m_1} (\delta_{t+m_1,0} + 1) (\delta_{t,0} + 1) (\delta_{s+m_1,0} + 1) (\delta_{s,0} + 1) \omega^{(t-s)n_1} \\
&\quad + \sum_{m_1, n_1} \omega^{m_1 m + n_1 n} \sum_{d-m_1 \leq t, s \leq d-1} (\delta_{t+m_1-d,0} + 1) (\delta_{s+m_1-d,0} + 1) \omega^{(t-s)n_1} \\
&\quad + \sum_{m_1, n_1} \omega^{m_1 m + n_1 n} \sum_{0 \leq t \leq d-1-m_1 < s \leq d-1} (\delta_{t+m_1,0} + 1) (\delta_{t,0} + 1) (\delta_{s+m_1-d,0} + 1) \zeta^{-d} \omega^{(t-s)n_1} \\
&\quad + \sum_{m_1, n_1} \omega^{m_1 m + n_1 n} \sum_{0 \leq s \leq d-1-m_1 < t \leq d-1} (\delta_{s+m_1,0} + 1) (\delta_{s,0} + 1) (\delta_{t+m_1-d,0} + 1) \zeta^d \omega^{(t-s)n_1} \\
&= S_1 + S_2 + S_3 + S_4
\end{aligned} \tag{C6}$$

In the following simplifications and subsequent derivations, we frequently make use of the identity

$$\sum_{t=0}^{d-1} t \omega^t = \frac{d}{\omega - 1}. \tag{C7}$$

This identity can be derived from the more general formula

$$\sum_{t=a}^b t x^t = x \left(\sum_{t=a}^b x^t \right)' = x \left(\frac{x^a - x^{b+1}}{1-x} \right)' = x \left(\frac{x^a - x^{b+1}}{(1-x)^2} + \frac{ax^{a-1} - (b+1)x^b}{1-x} \right), \quad \forall 0 \leq a \leq b, x \neq 1. \tag{C8}$$

In particular, setting $a = 0$, $b = d - 1$, and $x = \omega$ yields Eq. (C7), which plays an important role in evaluating the eigenvalues.

By detailed computation, we can obtain the following results.

$$\begin{aligned}
S_1 &= 2d^2 \delta_{m,0} \delta_{n,0} + 8d \delta_{n,0} + 4d + d \sum_{m_1=0}^{d-1-n} \omega^{m_1 m} \\
&\quad + d \sum_{m_1=0}^{n-1} \omega^{m_1 m} + dn \sum_{m_1=0}^{n-1} \omega^{m_1 m} - d \sum_{m_1=0}^{n-1} \omega^{m_1 m} m_1 + d \sum_{m_1=0}^{d-1-n} \omega^{m_1 m} (d - m_1 - n)
\end{aligned} \tag{C9}$$

$$\begin{aligned}
S_2 &= \delta_{n,0} d \sum_{m_1=1}^{d-1} \omega^{m_1 m} + d \sum_{m_1=n+1}^{d-1} \omega^{m_1 m} + \delta_{n,0} d \sum_{m_1=1}^{d-1} \omega^{m_1 m} \\
&\quad + d \sum_{m_1=d-n+1}^{d-1} \omega^{m_1 m} + d \sum_{m_1=n+1}^{d-1} \omega^{m_1 m} (m_1 - n) + d \sum_{m_1=d-n+1}^{d-1} \omega^{m_1 m} (n - d + m_1)
\end{aligned} \tag{C10}$$

Let $\tilde{n} := \min(n, d - n)$.

$$\begin{aligned}
S_3 = & d\zeta^{-d}(1 - \delta_{n,0})\omega^{-mn} + d\zeta^{-d} \sum_{m_1=d-n}^{d-1} \omega^{m_1 m} + d\zeta^{-d} \sum_{m_1=1}^{d-n} \omega^{m_1 m} \\
& + d\zeta^{-d} \sum_{m_1=1}^{\tilde{n}-1} \omega^{m_1 m} m_1 + d\zeta^{-d} \sum_{m_1=\tilde{n}}^{d-\tilde{n}} \omega^{m_1 m} \tilde{n} + d\zeta^{-d} \sum_{m_1=d-\tilde{n}+1}^{d-1} \omega^{m_1 m} (d - m_1)
\end{aligned} \tag{C11}$$

Note that

$$S_4 = S_3^*. \tag{C12}$$

Our current objective is to determine whether the total expression $S_1 + S_2 + S_3 + S_4$, defined in Eqs. (C9), (C10), (C11), and (C12), is nonzero in each of the following four cases: $(m \neq 0, n = 0)$, $(m \neq 0, n \neq 0)$, $(m = 0, n = 0)$, and $(m = 0, n \neq 0)$.

Case 1: We first consider the case $m \neq 0$. We have

$$S_1 = 8d\delta_{n,0} + 4d + \frac{d}{1 - \omega^m} (d + 2 - \omega^{-mn} - \omega^{mn}) - \frac{d\omega^m}{(1 - \omega^m)^2} (2 - \omega^{mn} - \omega^{-mn}), \tag{C13}$$

$$\begin{aligned}
S_2 = & -2d\delta_{n,0} + \frac{d}{1 - \omega^m} (2\omega^{m(n+1)} + n - d - 1) + \frac{d}{(1 - \omega^m)^2} (\omega^{m(n+2)} - \omega^m) \\
& + (1 - \delta_{n=0})d \left(\frac{2\omega^{m(1-n)} - n - 1}{1 - \omega^m} + \frac{\omega^m}{(1 - \omega^m)^2} (\omega^{m(1-n)} - 1) \right).
\end{aligned} \tag{C14}$$

and

$$S_3 = d\zeta^{-d} \left((2 - \delta_{n=0})\omega^{-mn} - 1 + \frac{\omega^m - \omega^{m(1-\tilde{n})}}{1 - \omega^m} + \frac{1}{(1 - \omega^m)^2} (\omega^m + \omega^{2m} - \omega^{m(1+\tilde{n})} - \omega^{m(2-\tilde{n})}) \right). \tag{C15}$$

• **Subcase 1:** $n = 0$

$$\begin{aligned}
& S_1 + S_2 + S_3 + S_4 \\
= & 8d + 4d + \frac{d^2}{1 - \omega^m} - 2d + \frac{d}{1 - \omega^m} (2\omega^m - d - 1) + \frac{d}{(1 - \omega^m)^2} (\omega^{2m} - \omega^m) \\
= & 9d > 0.
\end{aligned} \tag{C16}$$

• **Subcase 2:** $n \neq 0$

$$\begin{aligned}
& S_1 + S_2 + S_3 + S_4 \\
&= 4d + \frac{d}{1-\omega^m} (d+2-\omega^{-mn}-\omega^{mn}) - \frac{d\omega^m}{(1-\omega^m)^2} (2-\omega^{mn}-\omega^{-mn}) \\
&+ \frac{d}{1-\omega^m} (2\omega^{m(n+1)}+n-d-1) + \frac{d}{(1-\omega^m)^2} (\omega^{m(n+2)}-\omega^m) \\
&+ d \left(\frac{2\omega^{m(1-n)}-n-1}{1-\omega^m} + \frac{\omega^m}{(1-\omega^m)^2} (\omega^{m(1-n)}-1) \right) \\
&+ d\zeta^{-d} \left(2\omega^{-mn}-1 + \frac{\omega^m-\omega^{m(1-\bar{n})}}{1-\omega^m} + \frac{1}{(1-\omega^m)^2} (\omega^m+\omega^{2m}-\omega^{m(1+\bar{n})}-\omega^{m(2-\bar{n})}) \right) \\
&+ d\zeta^d \left(2\omega^{mn}-1 + \frac{\omega^{-m}-\omega^{-m(1-\bar{n})}}{1-\omega^{-m}} + \frac{1}{(1-\omega^{-m})^2} (\omega^{-m}+\omega^{-2m}-\omega^{-m(1+\bar{n})}-\omega^{-m(2-\bar{n})}) \right) \\
&= 4d + \frac{d}{1-\omega^m} (-\omega^{-mn}-\omega^{mn}+2\omega^{m(n+1)}+2\omega^{m(1-n)}) \\
&+ \frac{d}{(1-\omega^m)^2} (\omega^{m(n+2)}-4\omega^m+\omega^{m(n+1)}+\omega^{m(1-n)}+\omega^{m(2-n)}) \\
&+ d\zeta^{-d} \left(2\omega^{-mn}-1 + \frac{\omega^m-\omega^{m(1-\bar{n})}}{1-\omega^m} + \frac{1}{(1-\omega^m)^2} (\omega^m+\omega^{2m}-\omega^{m(1+\bar{n})}-\omega^{m(2-\bar{n})}) \right) \\
&+ d\zeta^d \left(2\omega^{mn}-1 + \frac{\omega^{m\bar{n}}-1}{1-\omega^m} + \frac{1}{(1-\omega^m)^2} (\omega^m+1-\omega^{m(1-\bar{n})}-\omega^{m\bar{n}}) \right) \\
&= 4d + \frac{4d+d(-\omega^{mn}-\omega^{-mn})(4-(\omega^m+\omega^{-m}))}{2-(\omega^m+\omega^{-m})} \\
&+ 2d(\zeta^{-d}\omega^{-mn}+\zeta^d\omega^{mn}) - d(\zeta^d+\zeta^{-d}) \left(1 + \frac{2-\omega^{-mn}-\omega^{mn}}{2-\omega^m-\omega^{-m}} \right)
\end{aligned} \tag{C17}$$

Let $\omega^m = e^{i\theta}$ and $\zeta = e^{i\alpha}$. Then

$$\begin{aligned}
& (S_1 + S_2 + S_3 + S_4)/d \\
&= 4 + 4 \cos(n\theta + \alpha) - 2 \cos \alpha - 2 \cos n\theta + (2 - \cos \alpha) \frac{1 - \cos n\theta}{1 - \cos \theta} > 0.
\end{aligned} \tag{C18}$$

(Note that as $\alpha \rightarrow 0$, the summation is $2 + 2 \cos n\theta + \frac{1 - \cos n\theta}{1 - \cos \theta} > 0$.)

Case 2: We then consider the case $m = 0$.

We have

$$S_1 = (2d^2 + 8d)\delta_{n=0} + \frac{1}{2}d^3 - nd^2 + dn^2 + \frac{3}{2}d^2 + 4d \tag{C19}$$

$$S_2 = 2\delta_{n,0}d(d-1) + d(d-n-1)\left(1 + \frac{d-n}{2}\right) + (1-\delta_{n,0})d(n-1)\left(1 + \frac{n}{2}\right), \tag{C20}$$

and

$$S_3 = d\zeta^{-d}((1-\delta_{n,0})(d-n+1) + n + nd - n^2). \tag{C21}$$

• **Subcase 1:** $n = 0$

$$\begin{aligned}
S_1 + S_2 + S_3 + S_4 &= (2d^2 + 8d) + \frac{1}{2}d^3 + \frac{3}{2}d^2 + 4d + 2d(d-1) + d(d-1)\left(1 + \frac{d}{2}\right) \\
&= d^3 + 6d^2 + 9d = d(d+3)^2 > 0.
\end{aligned} \tag{C22}$$

• **Subcase 2:** $n \neq 0$

$$\begin{aligned}
& S_1 + S_2 + S_3 + S_4 \\
&= \frac{1}{2}d^3 - nd^2 + dn^2 + \frac{3}{2}d^2 + 4d + d(d-n-1)\left(1 + \frac{d-n}{2}\right) + d(n-1)\left(1 + \frac{n}{2}\right) + d(\zeta^{-d} + \zeta^d)((d-n+1) + n + nd - n^2) \\
&= d(d^2 + 2n^2 - 2dn + 2d + 2 + (\zeta^d + \zeta^{-d})(1 + d + nd - n^2))
\end{aligned} \tag{C23}$$

We can find that $1 + d + nd - n^2 = (n+1)(d+1-n) > 0$. Since $-2 < \zeta^d + \zeta^{-d} < 2$, the summation

$$S_1 + S_2 + S_3 + S_4 > d(d^2 + 2n^2 - 2dn + 2d + 2 - 2(1 + d + nd - n^2)) = (d - 2n)^2 \geq 0. \tag{C24}$$

In all four cases $(m, n) \in \{(0, 0), (0, \neq 0), (\neq 0, 0), (\neq 0, \neq 0)\}$, we have verified that

$$S_1 + S_2 + S_3 + S_4 > 0.$$

□

3. IC Fiducial Construction for Odd Dimensions

We provide a construction of a fiducial state that generates an informationally complete POVM (IC-POVM) in any odd dimension d , and compute all eigenvalues of the resulting Gram matrix explicitly.

Statement 3. *Let d be an odd positive integer. Consider the unnormalized fiducial state $|\phi\rangle \in \mathbb{C}^d$ defined by*

$$|\phi\rangle = \sum_{j=0}^{d-1} (1 - \delta_{j,j_0})|j\rangle, \tag{C25}$$

where $j_0 \in \{0, 1, \dots, d-1\}$ specifies the index at which the coefficient is zero, and all other entries are set to 1.

Then, the Gram matrix $\mathcal{G}_{|\phi\rangle}$, defined via the Weyl–Heisenberg orbit of $|\phi\rangle$, has full rank. Consequently, the orbit generates an IC-POVM. Furthermore, all the eigenvalues λ_{mn} of $\mathcal{G}_{|\phi\rangle}$, as given in Eq. (B11), are strictly positive and explicitly take the form:

$$\lambda_{mn} = \begin{cases} d(d-1)^2, & \text{if } m = 0, n = 0; \\ d(d-2)^2, & \text{if } m = 0, n \neq 0; \\ d, & \text{if } m \neq 0, n = 0; \\ d(2 + \omega^{mn} + \omega^{-mn}), & \text{if } m \neq 0, n \neq 0. \end{cases}$$

Proof. We have

$$\begin{aligned}
& \lambda_{mn} \\
&= \sum_{m_1, n_1} \omega^{m_1 m + n_1 n} \left| \sum_t (1 - \delta_{t+m_1, s_0})(1 - \delta_{t, s_0}) \omega^{tn_1} \right|^2 \\
&= \sum_{m_1, n_1} \omega^{m_1 m + n_1 n} \left| d\delta_{n_1, 0} - \omega^{(s_0 - m_1)n_1} - \omega^{s_0 n_1} + \omega^{s_0 n_1} \delta_{m_1, 0} \right|^2 \\
&= \sum_{m_1, n_1} \omega^{m_1 m + n_1 n} \left(d\delta_{n_1, 0} - \omega^{(s_0 - m_1)n_1} - \omega^{s_0 n_1} + \omega^{s_0 n_1} \delta_{m_1, 0} \right) \left(d\delta_{n_1, 0} - \omega^{-(s_0 - m_1)n_1} - \omega^{-s_0 n_1} + \omega^{-s_0 n_1} \delta_{m_1, 0} \right) \\
&= \sum_{m_1, n_1} \omega^{m_1 m + n_1 n} (2d\delta_{\beta, 0} + (d^2 - 4d)\delta_{n_1, 0} - 3\delta_{m_1, 0} + \omega^{-m_1 n_1} + \omega^{m_1 n_1} + 2) \\
&= 2d + \sum_{m_1} \omega^{m_1 m} (d^2 - 4d) - \sum_{n_1} 3\omega^{n_1 n} + \sum_{m_1, n_1} \omega^{m_1 m + n_1 n} (\omega^{-m_1 n_1} + \omega^{m_1 n_1} + 2) \\
&= 2d + d^2(d-4)\delta_{m, 0} - 3d\delta_{n, 0} + 2d^2\delta_{m, 0}\delta_{n, 0} + d(\omega^{mn} + \omega^{-mn})
\end{aligned} \tag{C26}$$

In summary, we have

$$\lambda_{mn} = \begin{cases} d(d-1)^2, & \text{if } m=0, n=0; \\ d(d-2)^2, & \text{if } m=0, n \neq 0; \\ d, & \text{if } m \neq 0, n=0; \\ d(2 + \omega^{mn} + \omega^{-mn}), & \text{if } m \neq 0, n \neq 0. \end{cases}$$

In particular, if d is odd, the sum $\omega^{mn} + \omega^{-mn} > -2$ for all m, n . Hence all eigenvalues λ_{mn} is nonzero. \square

Remark 3. In the case where d is even, the above construction fails to produce an IC-POVM. This is because there exist indices m, n such that $mn = d/2$, leading to $\omega^{mn} = \omega^{-mn} = -1$. In this case, the corresponding eigenvalue becomes

$$\lambda_{mn} = d(2 + \omega^{mn} + \omega^{-mn}) = d(2 - 1 - 1) = 0,$$

which causes the Gram matrix $\mathcal{G}_{|\phi\rangle}$ to be rank-deficient and thus not enough informationally complete.

Remark 4. Since d is odd, we have

$$\min_{m,n} (\omega^{mn} + \omega^{-mn}) = 2 \min_{m,n} \cos \frac{2mn}{d} \pi = 2 \cos \left(\frac{d-1}{d} \pi \right) = -2 \cos(\pi/d). \quad (\text{C27})$$

Then the minimal eigenvalue is

$$\lambda_{\min} = \min_{m,n} d(2 + \omega^{mn} + \omega^{-mn}) = 2d(1 - \cos(\pi/d)) = \pi^2/d + O(d^{-3}) \quad (\text{C28})$$

Appendix D: Proof of Theorem 3:

In this appendix, we provide the proof of Theorem 3, which characterizes several classes of fiducial states whose Weyl–Heisenberg orbits fail to generate informationally complete POVMs. Each case is treated separately, based on the structure of the Gram matrix and the symmetries or sparsity properties of the chosen state.

Case 1: Real-valued state in even dimension

Statement 4. Let d be an even positive integer. Then for any pure quantum state $|\phi\rangle \in \mathbb{C}^d$ whose components are all real, the Gram matrix $\mathcal{G}_{|\phi\rangle}$ is rank-deficient, i.e., $\det(\mathcal{G}_{|\phi\rangle}) = 0$. Consequently, such a state cannot generate an IC-POVM via the Weyl–Heisenberg group action.

More specifically, for all odd integers $m \in \{1, 3, \dots, d-1\}$, we have

$$\lambda_{m,d/2} = 0,$$

where λ_{mn} are the eigenvalues of $\mathcal{G}_{|\phi\rangle}$ as defined in Eq. (B11).

Proof. For each $m \in \{1, 3, \dots, d-1\}$, we directly compute the corresponding eigenvalue:

$$\begin{aligned} \lambda_{m,d/2} &= \sum_{m_1, n_1} \omega^{mm_1 + dn_1/2} \left| \sum_t a_{t+m_1}^* a_t \omega^{n_1 t} \right|^2 \\ &= \sum_{m_1} \omega^{mm_1} \left[\sum_{t,s} a_{t+m_1} a_t a_{s+m_1} a_s \left(\sum_{n_1} \omega^{(t-s+d/2)n_1} \right) \right] \\ &= d \sum_{m_1} \omega^{mm_1} \sum_{t-s \equiv d/2} a_s a_t a_{s+m_1} a_{t+m_1} \\ &= d \sum_{m_1=0}^{d/2-1} \omega^{mm_1} \sum_s a_s a_{s+m_1} a_{s+d/2} a_{s+m_1+d/2} + d \sum_{m_1=d/2}^{d-1} \omega^{mm_1} \sum_s a_s a_{s+m_1} a_{s+d/2} a_{s+m_1+d/2} \\ &= d \sum_{m_1=0}^{d/2-1} \omega^{mm_1} \sum_s a_s a_{s+m_1} a_{s+d/2} a_{s+m_1+d/2} + d \sum_{m_1=0}^{d/2-1} \omega^{m(m_1+d/2)} \sum_s a_s a_{s+m_1} a_{s+d/2} a_{s+m_1} \end{aligned} \quad (\text{D1})$$

Since m is odd and d is even, we have $\omega^{md/2} = -1$, which implies that the total expression becomes zero:

$$\lambda_{m,d/2} = 0.$$

This completes the proof. \square

Remark 5. This result implies that for n -qubit systems (i.e., $d = 2^n$), in order to construct a fiducial state $|\phi\rangle$ such that $\det(\mathcal{G}_{|\phi\rangle}) \neq 0$, the corresponding quantum circuit preparing $|\phi\rangle$ from the initial state $|0\rangle^{\otimes n}$ cannot be composed solely of Hadamard gates, CNOT gates, and single-qubit rotations of the form $R_y(\theta)$. Such gate sets are restricted to generating quantum states with real amplitudes. However, our result shows that when d is even, any all-real fiducial state necessarily yields a rank-deficient Gram matrix.

Consequently, the prepared state must exhibit nontrivial relative phases between at least two computational basis components, typically requiring gate operations that introduce complex amplitudes (e.g., phase gates or arbitrary single-qubit unitaries with complex entries). In particular, some components must carry a relative phase of the form $e^{i\alpha}$, where $\alpha \notin \{0, \pi\}$.

Case 2: Root-of-unity coefficients

Statement 5. Let $|\phi\rangle = \frac{1}{\sqrt{d}} \sum_{k=0}^{d-1} a_k |k\rangle \in \mathbb{C}^d$ be a pure quantum state such that each coefficient a_k is a root of unity; that is, for each k , there exists a positive integer m_k such that $a_k^{m_k} = 1$. Then the Gram matrix $\mathcal{G}_{|\phi\rangle}$ generated by the Weyl–Heisenberg orbit of $|\phi\rangle$ is rank-deficient, i.e., $\det(\mathcal{G}_{|\phi\rangle}) = 0$. Hence, such a state cannot be used to construct an IC-POVM.

Proof. We can easily prove that when $m \neq 0$ and $n = 0$, the corresponding eigenvalues λ_{mn} all vanish, i.e., $\lambda_{mn} = 0$.

$$\begin{aligned} \lambda_{m,0} &= \sum_{m_1, n_1} \omega^{mm_1} \left| \sum_t a_{t+m_1}^* a_t \omega^{n_1 t} \right|^2 \\ &= \sum_{m_1} \omega^{mm_1} \sum_{t,s} a_{t+m_1}^* a_t a_{s+m_1} a_s^* d \delta_{t,s} \\ &= \sum_{m_1} \omega^{mm_1} \sum_t |a_{t+m_1} a_t|^2 d \\ &= \sum_{m_1} \omega^{mm_1} d^2 = d^3 \delta_{m,0}. \end{aligned} \tag{D2}$$

\square

Remark 6. This result implies that for n -qubit systems (i.e., $d = 2^n$), n -qubit stabilizer states $|\phi_n\rangle$ with all nonzero coefficients cannot serve as fiducial states for constructing IC-POVMs via Weyl–Heisenberg orbits. More broadly, any state obtained by applying a Clifford circuit composed of gates such as $\{S, T, X, CX, CZ\}$ to $|\phi_n\rangle$ will have components that are roots of unity. According to the above theorem, such states result in a rank-deficient Gram matrix and hence fail to generate an IC-POVM. Here, CX and CZ denote the controlled- X and controlled- Z operations, respectively.

Case 3: Sparse states with few nonzero components

Statement 6. Let $|\phi\rangle \in \mathbb{C}^d$ be a vector with exactly t_1 nonzero components, and let $t_0 = d - t_1$ denote the number of zero components. If $t_0 > d - \sqrt{d - \frac{3}{4}} - \frac{1}{2}$ (equivalently, if $t_1 < \sqrt{d - \frac{3}{4}} + \frac{1}{2}$), then the Gram matrix $\mathcal{G}_{|\phi\rangle}$ associated with the Weyl–Heisenberg orbit of $|\phi\rangle$ is rank-deficient. In particular, there exists some $n \in \{0, 1, \dots, d-1\}$ such that

$$\lambda_{mn} = 0, \quad \text{for all } m \in \{0, 1, \dots, d-1\}.$$

Consequently, such a state $|\phi\rangle$ cannot be used to construct an IC-POVM by Weyl–Heisenberg group.

Proof. Assume $|\phi\rangle = (a_0, \dots, a_{d-1})^t$ and $a_i \neq 0$ if and only if $i \in S := \{i_0, i_1, \dots, i_{t_1} - 1\}$. Then

$$\begin{aligned} \lambda_{mn} &= \sum_{0 \leq m_1, n_1 \leq d-1} \omega^{m_1 m + n_1 n} \left| \sum_{t \in S} a_{t+m_1}^* a_t \omega^{tn_1} \right|^2 \\ &= \sum_{n_1} \omega^{n_1 n} \sum_{m_1} \omega^{m_1 m} \left| \sum_{t \in S} a_{t+m_1}^* a_t \omega^{tn_1} \right|^2 \\ &= \sum_{n_1} \omega^{n_1 n} \sum_{m_1} \omega^{m_1 m} \left(\sum_{t' \in S} a_{t'+m_1}^* a_{t'} \omega^{t'n_1} \right) \left(\sum_{t \in S} a_{t+m_1} a_t^* \omega^{-tn_1} \right) \end{aligned}$$

Write $D(S) = \{i-j | i, j \in S\} \subset \{0, 1, \dots, d-1\}$ (if $i-j < 0$ we choose the integer $m \in \{0, 1, \dots, d-1\}$ s.t. $m \equiv i-j \pmod{d}$). Note that the above summation can be written as follows

$$\begin{aligned} \lambda_{mn} &= \sum_{n_1} \omega^{n_1 n} \sum_{t \in D(S)} c_t \omega^{tn_1} \\ &= \sum_{t \in D(S)} c_t \sum_{n_1} \omega^{n_1(n-t)} \end{aligned}$$

here $c_t \in \mathbb{C}$ are coefficients independent of n_1 . Since $\sum_{n_1} \omega^{tn_1} \neq 0$ if and only if $\omega^t = 1$, the summation $\lambda_{mn} = 0$ if $n \notin D(S)$. One can find that the cardinality $|D(S)| \leq 2 \binom{t_1}{2} + 1 = t_1^2 - t_1 + 1$. Hence,

$$|D(S)| \leq t_1^2 - t_1 + 1 < |\{0, 1, \dots, d-1\}| = d \quad (D3)$$

ensure that there exists $n \in \{0, 1, \dots, d-1\} \setminus D(S)$ s.t., $\lambda_{mn} = 0$ for all $m \in \{0, 1, \dots, d-1\}$. \square

Remark 7. The above statement establishes a necessary condition for a quantum state $|\phi\rangle \in \mathbb{C}^d$ to generate an IC-POVM via its Weyl–Heisenberg orbit: the number of nonzero components t_1 must satisfy

$$t_1 \geq \sqrt{d - \frac{3}{4}} + \frac{1}{2},$$

which is obtained by Eq. (D3). Equivalently, if the number of vanishing components $t_0 = d - t_1$ exceeds $d - \sqrt{d - \frac{3}{4}} - \frac{1}{2}$, the Gram matrix $\mathcal{G}_{|\phi\rangle}$ is rank-deficient, and the orbit fails to yield an IC-POVM.

This constraint has direct implications for common classes of quantum states. For instance, in n -qubit systems ($d = 2^n$), stabilizer states have support on $t_1 = 2^k$ computational basis states for some $0 \leq k \leq n$. To satisfy the above inequality, one must have

$$2^k \geq \sqrt{2^n - \frac{3}{4}} + \frac{1}{2},$$

which asymptotically requires $k \geq \lceil \frac{n+1}{2} \rceil$. In particular, stabilizer states with small support cannot generate IC-POVMs.

Furthermore, widely studied entangled states such as the Greenberger–Horne–Zeilinger (GHZ) state and the W state also fail to meet the condition: the GHZ state has only two nonzero components, and the W state has n nonzero components. Both are below the threshold for all $n \geq 1$, and hence cannot serve as fiducial states for constructing IC-POVMs through Weyl–Heisenberg group action.

Combining Statement 5, this implies that the exponent k in the n -qubit stabilizer support size must lie within the range $\lceil \frac{n+1}{2} \rceil, \dots, n-1$ in order for the state to potentially yield a full-rank Gram matrix.

Case 4: Qudit stabilizer states

In a d -dimensional Hilbert space, *qudit stabilizer states* are defined as the common $+1$ eigenstates of a maximal abelian subgroup of the Weyl–Heisenberg group. Equivalently, they can be characterized as the orbit of the computational basis state $|0\rangle$ under the action of the *Clifford group*, which is the normalizer of the Weyl–Heisenberg group in the unitary group $U(d)$. This construction generalizes the well-known Pauli–Clifford stabilizer formalism from qubit

systems ($d = 2$) to arbitrary finite dimensions, and plays a central role in non-binary quantum error correction and many-body quantum systems.

Despite their widespread usefulness, we show that such stabilizer states are intrinsically unsuitable for constructing informationally complete POVMs: for any d , the Gram matrix $\mathcal{G}_{|\phi\rangle}$ associated with the Weyl–Heisenberg orbit of a stabilizer state $|\phi\rangle$ is necessarily rank-deficient, i.e., $\det(\mathcal{G}_{|\phi\rangle}) = 0$. This implies that the orbit cannot span the full operator space and thus fails to form an informationally complete POVM (IC-POVM).

Statement 7. *Let $|\phi\rangle$ be any stabilizer state in a d -dimensional Hilbert space, defined as the common $+1$ eigenstate of a maximal abelian subgroup of the Weyl–Heisenberg group. Then the Gram matrix $\mathcal{G}_{|\phi\rangle}$, constructed from the Weyl–Heisenberg orbit of $|\phi\rangle$, is always rank-deficient. In particular,*

$$\det(\mathcal{G}_{|\phi\rangle}) = 0,$$

and the orbit cannot form an informationally complete POVM (IC-POVM).

Proof. Let $|\phi\rangle = U|0\rangle$ be a stabilizer state, where U is a Clifford unitary.

The Gram matrix $\mathcal{G}_{|\phi\rangle} \in \mathbb{R}^{d^2 \times d^2}$ is defined by

$$\mathcal{G}_{|\phi\rangle}(\alpha, \beta) = |\langle \phi | D_\alpha^\dagger D_\beta | \phi \rangle|^2,$$

where $D_\alpha = X^{j_\alpha} Z^{k_\alpha}$ denotes a Weyl–Heisenberg displacement operator, indexed by $\alpha = (j_\alpha, k_\alpha) \in \mathbb{Z}_d^2$.

Substituting $|\phi\rangle = U|0\rangle$ and using the fact that Clifford unitaries conjugate Weyl–Heisenberg operators into other Weyl–Heisenberg operators (i.e., $U^\dagger D_\alpha U = D'_\alpha \in \text{WH}$), we obtain

$$\mathcal{G}_{|\phi\rangle}(\alpha, \beta) = |\langle 0 | D'_\alpha{}^\dagger D'_\beta | 0 \rangle|^2.$$

Thus, $\mathcal{G}_{|\phi\rangle}$ is unitarily equivalent to $\mathcal{G}_{|0\rangle}$, up to a relabeling of the indices. That is, the eigenvalues of $\mathcal{G}_{|\phi\rangle}$ and $\mathcal{G}_{|0\rangle}$ are identical.

Now observe that the fiducial state $|0\rangle$ has only one nonzero component in the computational basis. According to Statement 6, any quantum state with fewer than $\sqrt{d - \frac{3}{4}} + \frac{1}{2}$ nonzero entries cannot generate an informationally complete POVM via the Weyl–Heisenberg orbit. Therefore, $\mathcal{G}_{|0\rangle}$ is necessarily rank-deficient, implying $\det(\mathcal{G}_{|0\rangle}) = 0$, and hence also $\det(\mathcal{G}_{|\phi\rangle}) = 0$.

We conclude that stabilizer states cannot be used to construct IC-POVMs via Weyl–Heisenberg orbits. \square

Appendix E: Proof of Theorem 4: Reconstruction from IC-POVMs by Weyl–Heisenberg orbit

Proof. Since the set $\{|\phi_\alpha\rangle\langle\phi_\alpha|\}$ forms an informationally complete frame, any density matrix ρ can be expanded as

$$\rho = \sum_{\alpha=0}^{d^2-1} a_\alpha |\phi_\alpha\rangle\langle\phi_\alpha| \quad (\text{E1})$$

for some coefficients $\{a_\alpha\}$.

Taking the trace with $|\phi_\beta\rangle\langle\phi_\beta|$ on both sides yields the linear system

$$p_\beta = \sum_{\alpha=0}^{d^2-1} \mathcal{G}_{|\phi\rangle}[\beta, \alpha] a_\alpha, \quad (\text{E2})$$

where $p_\beta = \text{tr}(\rho|\phi_\beta\rangle\langle\phi_\beta|)$ is the measurement probability, and $\mathcal{G}_{|\phi\rangle}[\beta, \alpha] = |\langle\phi_\beta|\phi_\alpha\rangle|^2$ is the Gram matrix element.

Since $\mathcal{G}_{|\phi\rangle}$ is Hermitian and admits a full spectral decomposition

$$\mathcal{G}_{|\phi\rangle} = \sum_{m,n=0}^{d-1} \lambda_{mn} |\Phi_{mn}\rangle\langle\Phi_{mn}|,$$

with strictly positive eigenvalues $\lambda_{mn} > 0$, it is invertible. Thus, the coefficients are given by

$$\mathbf{a} = \mathcal{G}_{|\phi\rangle}^{-1} \mathbf{p} = \sum_{m,n=0}^{d-1} \lambda_{mn}^{-1} \langle\Phi_{mn}|\mathbf{p}\rangle |\Phi_{mn}\rangle, \quad (\text{E3})$$

where $\mathbf{p} = (p_0, p_1, \dots, p_{d^2-1})^T$ and $\langle\Phi_{mn}|\mathbf{p}\rangle$ denotes the standard inner product.

Substituting the solved coefficients $\{a_\alpha\}$ into the expansion of ρ yields the desired reconstruction formula. \square

Appendix F: Proof of Classical Shadow Tomography Results

This appendix provides a complete derivation of the classical shadow tomography procedure using IC-POVMs generated by Weyl–Heisenberg orbits. We present the inverse channel construction, variance expressions, and both worst-case and average-case bounds.

1. Inverse Channel Construction

The quantum channel corresponding for the measurement is

$$F(\rho) = \sum_{k=0}^{d^2-1} \text{tr} \left(\frac{1}{d} |\phi_k\rangle\langle\phi_k| \rho \right) |\phi_k\rangle\langle\phi_k|. \quad (\text{F1})$$

We expand $\rho = \sum_{\alpha} a_{\alpha} |\phi_{\alpha}\rangle\langle\phi_{\alpha}|$. Applying the channel F to ρ gives

$$\begin{aligned} F(\rho) &= \sum_{k=0}^{d^2-1} \text{tr} \left(\frac{1}{d} |\phi_k\rangle\langle\phi_k| \rho \right) |\phi_k\rangle\langle\phi_k| \\ &= \frac{1}{d} \sum_{k=0}^{d^2-1} \text{tr} \left(|\phi_k\rangle\langle\phi_k| \sum_{\alpha=0}^{d^2-1} a_{\alpha} |\phi_{\alpha}\rangle\langle\phi_{\alpha}| \right) |\phi_k\rangle\langle\phi_k| \\ &= \frac{1}{d} \sum_{k=0}^{d^2-1} \left(\sum_{\alpha=0}^{d^2-1} a_{\alpha} \text{tr} (|\phi_k\rangle\langle\phi_k| |\phi_{\alpha}\rangle\langle\phi_{\alpha}|) \right) |\phi_k\rangle\langle\phi_k| \\ &= \frac{1}{d} \sum_{k=0}^{d^2-1} \left(\sum_{\alpha=0}^{d^2-1} a_{\alpha} |\langle\phi_k|\phi_{\alpha}\rangle|^2 \right) |\phi_k\rangle\langle\phi_k|. \end{aligned} \quad (\text{F2})$$

This implies the coefficient relation:

$$\mathbf{b} = \frac{1}{d} \mathcal{G} \mathbf{a}, \quad (\text{F3})$$

where \mathbf{b} and \mathbf{a} are the coefficient vectors of $F(\rho)$ and ρ under basis $\{|\phi_k\rangle\langle\phi_k|\}$ respectively, and $\mathcal{G}_{k\alpha} = |\langle\phi_k|\phi_{\alpha}\rangle|^2$ is the Gram matrix.

Since \mathcal{G} is invertible, we solve

$$\mathbf{a} = d \mathcal{G}^{-1} \mathbf{b}. \quad (\text{F4})$$

Thus, the inverse channel acting on a single outcome is:

$$F^{-1}(|\phi_k\rangle\langle\phi_k|) = d \sum_{\alpha=0}^{d^2-1} \mathcal{G}_{\alpha k}^{-1} |\phi_{\alpha}\rangle\langle\phi_{\alpha}|. \quad (\text{F5})$$

To estimate the expectation value of an observable O using classical shadows, it is essential to characterize the variance, which determines the required sample number of measurements.

2. Variance Expression and Worst-Case Bound

Given an unknown state σ , the variance is linearly related to

$$\|O_0\|_{\sigma}^2 = \sum_{k=0}^{d^2-1} \left(\text{tr} (F^{-1}(|\phi_k\rangle\langle\phi_k|) O_0) \right)^2 \text{tr} \left(\frac{|\phi_k\rangle\langle\phi_k|}{d} \sigma \right), \quad (\text{F6})$$

where $O_0 = O - \frac{\text{tr}(O)}{d} I$ denotes the traceless part of the observable.

By Eq. (F2), we have that the quantum channel F is represented as $[F] = \frac{1}{d}\mathcal{G}$ under the basis $\{|\phi_k\rangle\langle\phi_k|\}$. Consequently, the inverse channel F^{-1} satisfies $[F^{-1}] = d\mathcal{G}^{-1}$. Since \mathcal{G} is Hermitian and positive definite (due to the informational completeness of the POVM), its inverse \mathcal{G}^{-1} is also Hermitian and positive definite. Therefore, the channel F^{-1} is a Hermitian superoperator when viewed in this basis. Equivalently, using the self-adjoint property of F^{-1} , we can also write

$$\|O_0\|_\sigma^2 = \sum_{k=0}^{d^2-1} (\text{tr}(F^{-1}(O_0)|\phi_k\rangle\langle\phi_k|))^2 \text{tr}\left(\frac{|\phi_k\rangle\langle\phi_k|}{d}\sigma\right). \quad (\text{F7})$$

Given an observable O , we expand its traceless part $O_0 = O - \text{tr}(O)/d$ as

$$O_0 = \sum_{k=0}^{d^2-1} c_k |\phi_k\rangle\langle\phi_k|. \quad (\text{F8})$$

We know F^{-1} is a linear operation. Starting from the expansion of $F^{-1}(O_0)$ in the $\{|\phi_\alpha\rangle\langle\phi_\alpha|\}$ basis by Eq. (17):

$$F^{-1}(O_0) = d \sum_{\alpha=0}^{d^2-1} \left(\sum_{k=0}^{d^2-1} (\mathcal{G}^{-1})_{\alpha k} c_k \right) |\phi_\alpha\rangle\langle\phi_\alpha|, \quad (\text{F9})$$

we substitute this into the expression:

$$\begin{aligned} \text{tr}(F^{-1}(O_0)|\phi_k\rangle\langle\phi_k|) &= d \sum_{\alpha=0}^{d^2-1} \left(\sum_{j=0}^{d^2-1} (\mathcal{G}^{-1})_{\alpha j} c_j \right) \text{tr}(|\phi_\alpha\rangle\langle\phi_\alpha||\phi_k\rangle\langle\phi_k|) \\ &= d \sum_{\alpha=0}^{d^2-1} \left(\sum_{j=0}^{d^2-1} (\mathcal{G}^{-1})_{\alpha j} c_j \right) |\langle\phi_\alpha|\phi_k\rangle|^2. \end{aligned} \quad (\text{F10})$$

Introducing the Gram matrix \mathcal{G} with entries $\mathcal{G}_{\alpha k} = |\langle\phi_\alpha|\phi_k\rangle|^2$, we can write:

$$\text{tr}(F^{-1}(O_0)|\phi_k\rangle\langle\phi_k|) = d \sum_{j=0}^{d^2-1} c_j \left(\sum_{\alpha=0}^{d^2-1} (\mathcal{G}^{-1})_{\alpha j} \mathcal{G}_{\alpha k} \right). \quad (\text{F11})$$

Since $\mathcal{G}^{-1}\mathcal{G} = I$, we find

$$\sum_{\alpha=0}^{d^2-1} (\mathcal{G}^{-1})_{\alpha j} \mathcal{G}_{\alpha k} = \delta_{jk}. \quad (\text{F12})$$

Thus, the expression simplifies to

$$\text{tr}(F^{-1}(O_0)|\phi_k\rangle\langle\phi_k|) = d \times c_k. \quad (\text{F13})$$

Consequently, we have

$$(\text{tr}(F^{-1}(O_0)|\phi_k\rangle\langle\phi_k|))^2 = d^2 c_k^2. \quad (\text{F14})$$

Substituting the above formula, we have

$$\|O_0\|_\sigma^2 = d^2 \sum_{k=0}^{d^2-1} c_k^2 \text{tr}\left(\frac{|\phi_k\rangle\langle\phi_k|}{d}\sigma\right). \quad (\text{F15})$$

We have $\text{tr}(|\phi_k\rangle\langle\phi_k|\sigma) \leq 1$ for all quantum state σ . Therefore,

$$\|O_0\|_{\text{shadow}}^2 \leq d \cdot \sum_{k=0}^{d^2-1} c_k^2. \quad (\text{F16})$$

3. Connecting Worst-Case Variance to Gram Matrix Spectrum

Recall that we have the decomposition of O_0 in the $\{|\phi_k\rangle\langle\phi_k|\}$ basis:

$$O_0 = \sum_{\alpha=0}^{d^2-1} c_\alpha |\phi_\alpha\rangle\langle\phi_\alpha|.$$

Thus, the squared Hilbert-Schmidt norm of O_0 reads

$$\text{tr}(O_0^2) = \sum_{\alpha,\beta} c_\alpha c_\beta \text{tr}(|\phi_\alpha\rangle\langle\phi_\alpha||\phi_\beta\rangle\langle\phi_\beta|) = \sum_{\alpha,\beta} c_\alpha c_\beta |\langle\phi_\alpha|\phi_\beta\rangle|^2 = \mathbf{c}^\top \mathcal{G} \mathbf{c}. \quad (\text{F17})$$

If the minimal eigenvalue of \mathcal{G} are bounded by λ_{\min} , then we have $\mathcal{G} \geq \lambda_{\min} I$. By Eq. (F17), we have

$$\text{tr}(O_0^2) \geq \lambda_{\min} \sum_{k=0}^{d^2-1} c_k^2, \quad (\text{F18})$$

which implies

$$\sum_{k=0}^{d^2-1} c_k^2 \leq \frac{1}{\lambda_{\min}} \text{tr}(O_0^2). \quad (\text{F19})$$

Then by Eq. (F16), we have

$$\|O_0\|_{\text{shadow}}^2 \leq \frac{d}{\lambda_{\min}} \text{tr}(O_0^2). \quad (\text{F20})$$

□

4. Average-Case Variance Bound

Given an unknown input state σ , we consider the average-case scenario by taking $\sigma = \frac{I}{d}$, i.e., the maximally mixed state.

Starting from the definition, the shadow norm is

$$\|O_0\|_\sigma^2 = \sum_{k=0}^{d^2-1} (\text{tr}(F^{-1}(O_0)|\phi_k\rangle\langle\phi_k|))^2 \text{tr}\left(\frac{|\phi_k\rangle\langle\phi_k|}{d}\sigma\right). \quad (\text{F21})$$

Substituting $\sigma = \frac{I}{d}$, we have

$$\text{tr}\left(\frac{|\phi_k\rangle\langle\phi_k|}{d}\sigma\right) = \frac{1}{d} \text{tr}\left(\frac{|\phi_k\rangle\langle\phi_k|}{d}\right) = \frac{1}{d^2}.$$

Thus, the average-case shadow norm becomes

$$\|O_0\|_{\text{average}}^2 = \frac{1}{d^2} \sum_{k=0}^{d^2-1} (\text{tr}(F^{-1}(O_0)|\phi_k\rangle\langle\phi_k|))^2. \quad (\text{F22})$$

Using Eq. (F14), we substitute into the expression and obtain

$$\begin{aligned} \|O_0\|_{\text{average}}^2 &= \frac{1}{d^2} \sum_{k=0}^{d^2-1} d^2 c_k^2 \\ &= \sum_{k=0}^{d^2-1} c_k^2 \leq \frac{1}{\lambda_{\min}} \text{tr}(O_0^2). \end{aligned} \quad (\text{F23})$$

Appendix G: Eigenvalue Bounds of the Gram Matrix

We provide the derivation of the spectral bounds presented in Property 2. First, by definition, the eigenvalues $\lambda_{m,n}$ of the Gram matrix satisfy

$$\lambda_{m,n} = \sum_{j,k=0}^{d-1} |\langle \phi | X^j Z^k | \phi \rangle|^2 \cdot \omega^{mj+nk},$$

where $\omega = e^{2\pi i/d}$. This is precisely the 2D discrete Fourier transform of the squared overlaps.

Note that the trace of the Gram matrix $\mathcal{G}_{|\phi\rangle}$ is simply the sum of all diagonal elements, each equal to 1:

$$\text{tr}(\mathcal{G}_{|\phi\rangle}) = \sum_{k=0}^{d^2-1} \langle \phi_k | \phi_k \rangle = d^2.$$

Therefore, the sum of all eigenvalues is also d^2 .

Furthermore, the component $\lambda_{0,0}$ satisfies

$$\lambda_{0,0} = \sum_{j,k} |\langle \phi | X^j Z^k | \phi \rangle|^2 = d.$$

It is because that the Weyl–Heisenberg orbit forms a tight frame with frame constant d .

Hence, the maximal possible value of λ_{\min} under the constraint $\sum_{m,n} \lambda_{m,n} = d^2$, with one known eigenvalue being d , is achieved when all other $d^2 - 1$ eigenvalues are equal:

$$\lambda_{\min} \leq \frac{d^2 - d}{d^2 - 1} = \frac{d}{d + 1}.$$

In summary, the minimum eigenvalue λ_{\min} of the Gram matrix satisfies

$$0 \leq \lambda_{\min} \leq \frac{d}{d + 1},$$

where both bounds are tight. The upper bound is attained when the fiducial state generates a SIC-POVM. Our numerical analysis reveals that even non-SIC fiducial states can saturate this upper bound, offering a new perspective on the spectral behavior of approximate constructions. On the other hand, the lower bound $\lambda_{\min} = 0$ occurs precisely when the Weyl–Heisenberg orbit fails to form an informationally complete POVM. \square

Appendix H: Eigenvalue Structure of the Gram Matrix for SIC-POVMs

Let $\{|\phi_k\rangle\}_{k=1}^{d^2}$ be a symmetric informationally complete set of pure states (SIC-POVM) in a Hilbert space of dimension d . These states satisfy the following inner product condition:

$$|\langle \phi_j | \phi_k \rangle|^2 = \begin{cases} 1, & \text{if } j = k, \\ \frac{1}{d+1}, & \text{if } j \neq k. \end{cases}$$

Let $\mathcal{G} \in \mathbb{R}^{d^2 \times d^2}$ denote the Gram matrix of squared inner products:

$$\mathcal{G}_{jk} = |\langle \phi_j | \phi_k \rangle|^2.$$

Then \mathcal{G} takes the following form:

$$\mathcal{G} = \left(1 - \frac{1}{d+1}\right) I_{d^2} + \frac{1}{d+1} \mathbf{1},$$

where $\mathbf{1} \in \mathbb{R}^{d^2 \times d^2}$ is the all-ones matrix, and I_{d^2} is the identity.

This is a classic form of a rank-one perturbation of a scalar matrix, and its eigenvalues can be computed explicitly: The all-ones matrix $\mathbf{1}$ has eigenvalue d^2 corresponding to the eigenvector $v = (1, 1, \dots, 1)^\top$, and 0 for all orthogonal directions. Therefore, the Gram matrix \mathcal{G} has the following eigenvalue structure: One eigenvalue:

$$\lambda_1 = \left(1 - \frac{1}{d+1}\right) + \frac{d^2}{d+1} = d,$$

and the remaining $d^2 - 1$ eigenvalues:

$$\lambda_{\min} = \left(1 - \frac{1}{d+1}\right) = \frac{d}{d+1}.$$

Hence, the full spectrum of \mathcal{G} is:

$$\text{Spec}(\mathcal{G}) = \left\{d, \frac{d}{d+1}, \dots, \frac{d}{d+1}\right\},$$

with multiplicities 1 and $d^2 - 1$, respectively. In particular, the smallest eigenvalue is

$$\lambda_{\min} = \frac{d}{d+1}.$$

This spectral property plays a key role in minimizing variance in classical shadow tomography using SIC-POVMs. \square

- [1] Ugo Fano. Description of states in quantum mechanics by density matrix and operator techniques. *Reviews of modern physics*, 29(1):74, 1957.
- [2] Andrew J Scott. Tight informationally complete quantum measurements. *Journal of Physics A: Mathematical and General*, 39(43):13507, 2006.
- [3] Hsin-Yuan Huang, Richard Kueng, and John Preskill. Predicting many properties of a quantum system from very few measurements. *Nature Physics*, 16(10):1050–1057, 2020.
- [4] Andrew Zhao, Nicholas C Rubin, and Akimasa Miyake. Fermionic partial tomography via classical shadows. *Physical Review Letters*, 127(11):110504, 2021.
- [5] Hong-Ye Hu and Yi-Zhuang You. Hamiltonian-driven shadow tomography of quantum states. *Physical Review Research*, 4(1):013054, 2022.
- [6] Hong-Ye Hu, Soonwon Choi, and Yi-Zhuang You. Classical shadow tomography with locally scrambled quantum dynamics. *Physical Review Research*, 5(2):023027, 2023.
- [7] Ahmed A Akhtar, Hong-Ye Hu, and Yi-Zhuang You. Scalable and flexible classical shadow tomography with tensor networks. *Quantum*, 7:1026, 2023.
- [8] Matteo Ippoliti, Yaodong Li, Tibor Rakovszky, and Vedika Khemani. Operator relaxation and the optimal depth of classical shadows. *Physical Review Letters*, 130(23):230403, 2023.
- [9] Kaifeng Bu, Dax Enshan Koh, Roy J Garcia, and Arthur Jaffe. Classical shadows with pauli-invariant unitary ensembles. *npj Quantum Information*, 10(1):6, 2024.
- [10] Yu Wang and Wei Cui. Classical shadow tomography with mutually unbiased bases. *Physical Review A*, 109(6):062406, 2024.
- [11] Maxwell West, Antonio Anna Mele, Martin Larocca, and Marco Cerezo. Real classical shadows. *Journal of Physics A: Mathematical and Theoretical*, 2024.
- [12] Christian Berton, Jonas Haferkamp, Marcel Hinsche, Marios Ioannou, Jens Eisert, and Hako Pashayan. Shallow shadows: Expectation estimation using low-depth random clifford circuits. *Physical Review Letters*, 133(2):020602, 2024.
- [13] Robbie King, David Gosset, Robin Kothari, and Ryan Babbush. Triply efficient shadow tomography. In *Proceedings of the 2025 Annual ACM-SIAM Symposium on Discrete Algorithms (SODA)*, pages 914–946. SIAM, 2025.
- [14] Atithi Acharya, Siddhartha Saha, and Anirvan M Sengupta. Shadow tomography based on informationally complete positive operator-valued measure. *Physical Review A*, 104(5):052418, 2021.
- [15] H Chau Nguyen, Jan Lennart Bönsel, Jonathan Steinberg, and Otfried Gühne. Optimizing shadow tomography with generalized measurements. *Physical Review Letters*, 129(22):220502, 2022.
- [16] Luca Innocenti, Salvatore Lorenzo, Ivan Palmisano, Francesco Albarelli, Alessandro Ferraro, Mauro Paternostro, and G Massimo Palma. Shadow tomography on general measurement frames. *PRX Quantum*, 4(4):040328, 2023.
- [17] Laurin E Fischer, Timothée Dao, Ivano Tavernelli, and Francesco Tacchino. Dual-frame optimization for informationally complete quantum measurements. *Physical Review A*, 109(6):062415, 2024.

- [18] Joseph M Renes, Robin Blume-Kohout, Andrew J Scott, and Carlton M Caves. Symmetric informationally complete quantum measurements. *Journal of Mathematical Physics*, 45(6):2171–2180, 2004.
- [19] Paweł Horodecki, Łukasz Rudnicki, and Karol Życzkowski. Five open problems in quantum information theory. *PRX Quantum*, 3(1):010101, 2022.
- [20] David Marcus Appleby, Hulya Yadsan-Appleby, and Gerhard Zauner. Galois automorphisms of a symmetric measurement. *arXiv preprint arXiv:1209.1813*, 2012.
- [21] Ingemar Bengtsson. Sics: some explanations. *Foundations of Physics*, 50:1794–1808, 2020.
- [22] Marcus Appleby, Steven T Flammia, and Gene S Kopp. A constructive approach to zauner’s conjecture via the stark conjectures. *arXiv preprint arXiv:2501.03970*, 2025.
- [23] Jonathan Jedwab and Amy Wiebe. A simple construction of complex equiangular lines. In *Algebraic Design Theory and Hadamard Matrices: ADTHM, Lethbridge, Alberta, Canada, July 2014*, pages 159–169. Springer, 2015.
- [24] Ingemar Bengtsson and Karol Życzkowski. *Geometry of quantum states: an introduction to quantum entanglement*. Cambridge university press, 2017.
- [25] Zilin Jiang, Jonathan Tidor, Yuan Yao, Shengtong Zhang, and Yufei Zhao. Equiangular lines with a fixed angle. *Annals of Mathematics*, 194(3):729–743, 2021.
- [26] Meng Cao, Tenghui Deng, and Yu Wang. Dynamical quantum state tomography with time-dependent channels. *Journal of Physics A: Mathematical and Theoretical*, 57(21):215301, 2024.